

Published in final edited form as:

Free Radic Biol Med. 2009 December 1; 47(11): 1539–1552. doi:10.1016/j.freeradbiomed.2009.09.003.

Isolevuglandins covalently modify phosphatidylethanolamines in vivo: detection and quantitative analysis of hydroxylactam adducts

Wei Li^a, James M. Laird^a, Liang Lu^a, Sanjoy Roychowdhury^c, Laura E. Nagy^{b,c,d}, Rong Zhou^a, John W. Crabb^{a,e}, and Robert G. Salomon^a

^aDepartment of Chemistry, Case Western Reserve University, Cleveland, Ohio

^bDepartment of Nutrition, Case Western Reserve University, Cleveland, Ohio

^cDepartment of Pathobiology, Cleveland Clinic Foundation, Cleveland, Ohio

^dDepartment of Gastroenterology, Cleveland Clinic Foundation, Cleveland, Ohio

^eCole Eye Institute, Cleveland Clinic Foundation, Cleveland, Ohio

Abstract

Levuglandins (LGs) and isolevuglandins (isoLGs, also called “isoketals” or “isoKs”) are extraordinarily reactive products of cyclooxygenase and free radical-induced oxidation of arachidonates. We now report the detection *in vivo* and quantitative analysis of LG/isoLG adducts that incorporate the amino group of phosphatidylethanolamines (PEs) into LG/isoLG-hydroxylactams. Notably, LC-MS/MS detection of these hydroxylactams is achieved with samples that are an order of magnitude smaller and sample processing is much simpler and less time-consuming than required for measuring protein-derived LG/isoLG-lysyl-lactams. A key feature of our protocol is treatment of biological phospholipid extracts with phospholipase A₂ to generate mainly 1-palmitoyl-2-lysoPE-hydroxylactams from heterogeneous mixtures of phospholipids with a variety of acyl groups on the 2-position. Over 160% higher mean levels of LG/isoLG-PE-hydroxylactam ($P < 0.001$) were detected in liver from chronic ethanol-fed mice (32.4 ± 6.3 ng/g, $n = 6$) compared to controls (12.1 ± 1.5 ng/g, $n = 4$), and mean levels in plasma from patients with age-related macular degeneration (5.2 ± 0.4 ng/ml, $n = 15$) were elevated ~53% ($P < 0.0001$) compared to healthy volunteers (3.4 ± 0.1 ng/ml, $n = 15$). Just as LG/isoLG-protein adducts provide a dosimeter of oxidative injury, this study suggests that LG/isoLG-PE-hydroxylactams are potential biomarkers for assessing risk for oxidative stress-stimulated diseases.

Keywords

levuglandin; LG; isolevuglandin; isoLG; isoketal; isoK; phosphatidylethanolamine; oxidative stress; biomarker; free radical; mass spectrometry; protein adduct

© 2009 Elsevier Inc. All rights reserved.

Address correspondence to: Robert G. Salomon, Department of Chemistry, Case Western Reserve University, Cleveland, OH 44106, Tel: 216-368-2592, Fax: 216-368-3006, rgs@po.cwru.edu.

Publisher's Disclaimer: This is a PDF file of an unedited manuscript that has been accepted for publication. As a service to our customers we are providing this early version of the manuscript. The manuscript will undergo copyediting, typesetting, and review of the resulting proof before it is published in its final citable form. Please note that during the production process errors may be discovered which could affect the content, and all legal disclaimers that apply to the journal pertain.

Introduction

Levuglandins (LGs) and isolevuglandins (isoLGs) are a family of reactive oxidized lipids formed by rearrangement of endoperoxide intermediates generated, respectively, through the cyclooxygenase and free radical-induced cyclooxygenation of arachidonates [1–5] (Fig.1). IsoLGs have alternatively been named “isoketals” or “isoKs” to “distinguish them from levuglandins formed by rearrangement of the cyclooxygenase endoperoxide intermediate, PGH₂” [6]. We avoid this alternative nomenclature because isoLGs are not ketals. Furthermore, the distinction is erroneous because the exact same levuglandin molecules, LGE₂ and LGD₂, are generated by both the cyclooxygenase and isoprostane pathways. The cyclooxygenase pathway generates only a single enantiomer of each product whereas, in the free radical-induced autoxidation of arachidonates (the isoprostane pathway), a racemic mixture of stereo and structural isomers (Fig. 1) is cogenerated with LGE₂ and LGD₂. The γ -ketoaldehyde functionality of the LGs and isoLGs makes them extraordinarily reactive towards primary amino groups in biomolecules. LGs and isoLGs react with the -amino groups of lysyl residues in proteins to produce covalent adducts with greater avidity than most other lipid oxidation products, e.g., 4-hydroxynonenal (4-HNE) or malondialdehyde (MDA) [4,7]. This feature makes covalent LG/isoLG adducts attractive as biomarkers to evaluate oxidative injury in the tissues. LGs/isoLGs initially react with the primary amino groups to form Schiff base adducts within seconds, that are transformed to pyrrole adducts in minutes [8]. However, these highly alkylated pyrroles are chemically sensitive compounds in the presence of oxygen [9] and are further oxidized in a few hours to stable end products, lactams and hydroxylactams (HLs) [10]. Our previous work showed that isoLGE₂-protein [3,11], iso[4]LGE₂-protein [12] and iso[7]LGD₂-protein [13] adducts are generated upon oxidation of low density lipoprotein (LDL) *in vitro*. First detected *in vivo* by immunoassays [14,15], quantitative analysis of LG/isoLG protein adducts has also been achieved by LC-MS/MS analysis of the LG/isoLG-lysyl-lactams generated by proteolysis of the protein adducts [16]. The levels of isoLG-protein adducts are elevated in diseases associated with oxidative injury [15,17–21]. Besides its potential utility as a marker of oxidative injury, covalent modification of biomolecules by LGs or isoLGs may have pathological consequences owing to interference with their functions. For example, LGs crosslink proteins with DNA [22] and interfere with mitosis through covalent adduction with tubulin preventing the formation of microtubules [23].

The primary amino groups of phosphatidylethanolamines (PEs) are targets for covalent modification by carbohydrates and lipid peroxidation products. PEs modified by aldehydes generated *in vivo*, such as 4-hydroxy-2-nonenal (HNE) [24] and acrolein [25], have been reported in recent years. In a model study, 1-palmitoyl-2-linoleoyl-sn-glycero-3-phosphoethanolamine was modified by LGE₂ analogously to the well-known reaction of protein lysyl residues with LGs, producing Schiff base and pyrrole derivatives that were stabilized by sodium borohydride reduction under argon protection [26]. On the basis of these findings, we predicted that *in vivo* in the presence of oxygen, LGs/isoLGs would modify PEs generating stable covalent lactam or hydroxylactam (HL) adducts (Fig.1).

In this study, using a method based on reverse phase high performance liquid chromatography with on-line electrospray ionization tandem mass spectrometry, we confirmed that iso[4]LGE₂ covalently binds ethanolamine phospholipids *in vitro* to form covalent pyrrole adducts that are oxidized in air to deliver stable lactam and HL adducts. These adducts could not be detected in biological samples. Because such adducts were expected to be present as a complex mixture in which the levels of individual species might not be sufficient for detection, we simplified the mixture by selective hydrolysis. In the event, phospholipase A₂ (PLA₂)-catalyzed hydrolysis of putative isoLG-diacyl-PE precursors in lipid extracts from human plasma and mouse liver allowed the detection of isoLG-lysoPE-HL derivatives of isoLGs. To prevent *in vitro* oxidation, a transition metal ion chelator (EDTA) and the antioxidant BHT

were present at all stages of sample processing [27]. This finding provides the key to a sensitive and rapid method for quantifying the level of LG/isoLG modification of ethanolamine phospholipids present *in vivo*. Notably, LC-MS/MS detection of isoLG-lysoPE-HLs is readily achieved with samples that are an order of magnitude smaller – e.g., 200 μ l human plasma samples and 10 mg samples of mouse liver – and sample processing is much simpler and less time-consuming than required for measuring protein-derived LG/isoLG-lysyl-lactams. These features enhance the potential clinical utility of LG/isoLG-PE-HLs for assessing oxidative injury.

Materials and methods

A protocol listing reagents and equipment, detailing equipment and reagent set-up, and step-by-step procedures for sample preparation and analysis is provided in the supplementary material pages 15–20.

Materials

1-Palmitoyl-2-hydroxy-*sn*-glycero-3-phosphoethanolamine (lyso-PE), 1,2-dipalmitoyl-D62-*sn*-glycero-3-phosphoethanolamine (D62-dP-PE) and 1-palmitoyl-2-arachidonoyl-*sn*-glycero-3-phosphocholine (PA-PC) were purchased from Avanti Polar Lipids (Alabaster, AL). Phospholipase A₂ (PLA₂, 10,000 units/ml) from porcine pancreas (P0861) was obtained from Sigma-Aldrich (St. Louis, MO). Myeloperoxidase (MPO) was purchased from Calbiochem (La Jolla, CA). All other chemicals were purchased from Sigma-Aldrich. HPLC solvents were purchased from Aldrich (Milwaukee, WI) or Fisher Scientific (Pittsburgh, PA). Bicinchoninic acid (BCA) Protein Assay Reagent was purchased from Pierce (Rockford, IL). Female C57BL/6 mice (8–10 weeks old) were purchased from Jackson Labs (Bar harbor, ME). All reverse phase high-performance liquid chromatography (HPLC) columns were obtained from Phenomenex (Torrance, CA). Iso[4]LGE₂ was prepared by Dr. James Laird as described elsewhere [28].

Plasma from age-related macular degeneration and control patients

Clinically documented age-related macular degeneration and control blood donors were obtained from the Cole Eye Institute, Cleveland Clinic Foundation with Institutional Review Board approval and according to Declaration of Helsinki principles. All patients received a comprehensive eye examination by a clinician in the Clinical Genomic and Proteomic AMD Study Group [29] and provided written informed consent. Human identifiers were removed and the specimens encoded by the Clinical Study Group to protect donor confidentiality. Disease progression was categorized based on fundus examination and advanced age-related macular degeneration patients with choroidal neovascularization ($n = 15$) were included in the study. Control donors ($n = 15$) lacked macular drusen and exhibited no clinical evidence of any retinal disorder. On average age-related macular degeneration blood donors were 72.7 years old (range 64–84) and control donors were 72.4 years old (range 52–80); both cohorts included 7 female and 8 male donors. Plasma was prepared as described elsewhere [29,30] in the presence of the antioxidant butylated hydroxytoluene (BHT; 22 μ g/ml plasma) and a protease inhibitor cocktail (Sigma product number P 8340; 10 μ l/ml plasma), quench frozen in liquid nitrogen and stored at -80°C under argon until analysis. All plasma samples were frozen and thawed only once.

General methods

Proton magnetic resonance (^1H NMR) spectra were recorded on Varian Inova AS400 spectrometer operating at 400 MHz. Proton chemical shifts are reported in parts per million (ppm) on the δ scale relative to deuterated chloroform ($\text{CDCl}_3, \delta 7.24$). Carbon magnetic resonance (^{13}C NMR) spectra were recorded on Varian Inova AS400 spectrometer at 100 MHz

and chemical shifts are reported relative to CDCl_3 (δ 77.0). All high resolution mass spectra were recorded on a Kratos AEI MS25 RFA high resolution mass spectrometer at 20 eV.

Chemical synthesis of iso[4]LGE₂-lysoPE-hydroxylactam

A solution containing iso[4]LGE₂ (5 mM), 1-palmitoyl-2-hydroxy-*sn*-glycero-3-phosphatidylethanolamine (5 mM), and triethylamine (50 mM) in 1 ml of chloroform/methanol/water (60:35:5, v/v/v) was incubated with magnetic stirring under an oxygen atmosphere for 12 h at room temperature. The reaction was quenched by adding saturated aqueous ammonium chloride (500 μ l). Then the mixture was extracted with methanol/chloroform (1:2, v/v, 3 \times 1.5 ml), and the organic layer was concentrated to afford crude product. HPLC separation of the reaction products was performed using a 600 solvent delivery system (Waters) coupled to a 717 autosampler (Waters), a 2996 photodiode array detector (Waters) and a SEDEX 75 evaporative light scattering detector (Sedere, France) using a semi-preparative Luna C18 (2) column (250 \times 10 mm, 5 μ m, Phenomenex). The mobile phase was created by mixing water/methanol (50:50, v/v) with 1 mM ammonium acetate (A) and water/methanol (5:95, v/v) (B) at a flow rate of 2 ml/min with the following gradient: 0–10 min A/B 100:0, 10–20 min a linear gradient from 100:0 to 50:50, 20–45 min 50:50, 45–46 min a linear gradient from 50:50 to 0:100, 47–77 min 0:100, 77–78 min a linear gradient from 0:100 to 100:0, 78–90 min 100:0. A fraction containing the hydroxylactam was collected from 59 to 61 min and characterized by hydrogen and carbon NMR (Fig. S1 and S2). ¹H NMR (400 MHz, CDCl_3), δ 7.12–6.94 (1H), 6.58–6.39 (1H), 5.72–5.55 (1H), 5.40–5.28 (1H), 4.43–3.88 (8H), 3.58–3.39 (1H), 3.39–3.20 (1H), 2.68–2.41 (6H), 2.12–1.94 (4H), 1.81–1.52 (7H), 1.05–1.39 (30H), 0.86 (t, 6H, J = 6.8 Hz). ¹³C NMR (100 MHz, CDCl_3), δ 176.20 (CO), 172.10 (CO), 171.95 (CO), 170.82 (CO), 155.91(C), 155.82(C), 137.97 (CH), 135.42 (CH), 135.20 (CH), 126.23 (CH), 126.20 (CH), 124.38 (CH), 124.34 (CH), 120.12 (CH), 119.88 (CH), 87.50 (C), 87.39 (C), 72.14 (CH), 72.02 (CH), 66.03 (CH₂), 65.52 (CH₂), 64.41 (CH₂), 63.43 (CH₂), 47.12 (CH₂), 39.21 (CH₂), 35.98 (CH₂), 32.22 (CH₂), 32.07 (CH₂), 29.43 (CH₂), 28.95 (CH₂), 28.50 (CH₂), 24.55 (CH₂), 24.21 (CH₂), 22.67 (CH₂), 22.02 (CH₂), 14.07 (CH₂).

Mass spectrometric characterization of the iso[4]LGE₂-lyso-PE-HL is presented in the “Results and Discussion” section together with that of the corresponding pyrrole and lactam adducts present in the reaction product mixture. To determine the yields of these iso[4]LGE₂ adducts, a calibration curve for the HL was generated from mixtures containing a fixed amount (2 ng) of internal standard (iso[4]LGE₂-D31-lyso-PE-HL) and various amounts of the iso[4]LGE₂-lysoPE-HL, and plotting peak area ratio vs analyte concentration ($y = 0.1100x + 0.0062$, $R^2 = 0.9995$). The yield of hydroxylactam adduct is 36%. Yields of lactam (26%) and pyrrole (2%) adducts were approximated using the hydroxylactam calibration curve.

Chemical synthesis of iso[4]LGE₂-D31lysoPE-HL internal standard

Iso[4]LGE₂-D62-DPPE-HL was prepared analogously as synthesis of iso[4]LGE₂-lysoPE-HL using 1,2-di-D31-palmitoyl-*sn*-glycero-3-phosphoethanolamine (D62-DPPE) in place of 1-palmitoyl-2-hydroxy-*sn*-glycero-3-phosphoethanolamine. Iso[4]LGE₂-D31-lysoPE-HL was then obtained by selective lipolysis catalyzed by PLA₂. A solution in methanol of crude iso[4]LGE₂-D62-DPPE-HL (100 μ l containing 50 mg/ml) was added to phosphate buffered saline (PBS, 1ml, 10 mM, pH 7.4) containing CaCl₂ (5 mM). The resulting mixture was sonicated for 10 min followed by the addition of PLA₂ (100 μ l). The resulting mixture was incubated at 37 °C for 10 h under argon. Then the product mixture was extracted three times with (3 \times 1.5 ml) methanol/chloroform (1:2, v/v). Solvents were evaporated from the organic layer under a stream of dry argon. The residue was dissolved in methanol/water (1:1, v/v) and subjected to the same protocol of HPLC separation as described above for purification of iso[4]LG-lysoPE-HL. Pure iso[4]LGE₂-D31-lysoPE-HL was isolated in 23% overall yield and characterized by proton NMR (Fig. S3) and mass spectrometry (Fig. S4). ¹H NMR (400 MHz, CDCl_3), δ

7.14-6.95 (1H), 6.59-6.35 (1H), 5.66-5.54 (1H), 5.39-5.31 (1H), 4.30-3.82 (8H), 3.59-3.14 (2H), 2.38-2.23 (6H), 2.09-1.93 (2H), 1.92-1.39 (5H), 1.31-1.10 (6H), 0.87 (t, 3H, J = 6.8 Hz).

Time course of the reaction between iso[4]LGE₂ and lyso-PE

The time course of the reaction between iso[4]LGE₂ and lyso-PE was determined. Synthetic iso[4]LGE₂ (5 mM) was incubated with 1-palmitoyl-2-hydroxy-*sn*-glycero-3-phosphatidylethanolamine (5 mM) in chloroform/methanol/water (2 ml of 60:35:5, v/v/v) containing triethylamine (50 mM). The mixture was stirred under an oxygen atmosphere at room temperature. Aliquots (200 μ l) were withdrawn at various times, and the reaction was quenched by adding 100 μ l of saturated aqueous ammonium chloride. Then the resulting mixture was extracted with methanol/chloroform (1:2, v/v, 3 \times 1.5 ml) and the organic layer was concentrated to afford crude product, which was analyzed by LC-MS/MS.

Free radical induced oxidation of PA-PC with lyso-PE

Small unilamellar vesicles comprised of PA-PC (0.2 mg/ml) and lyso-PE (0.8 mg/ml) were prepared by extrusion (10 times) through a 0.1 μ m polycarbonate filter using an Avanti Mini-Extruder (Avanti Polar Lipids, Inc., Alabaster, AL) in argon-sparged phosphate buffered saline (PBS, 50 mM, pH 7.0, supplemented with 200 μ M diethylenetriamine pentaacetic acid, (DTPA)) [31]. The vesicles were oxidized by exposure to glucose oxidase (100 ng/ml), glucose (100 μ g/ml), sodium nitrite (500 μ M) and myeloperoxidase (MPO, 30 nM) as described previously [32]. The small unilamellar vesicles solution (2.5 ml) was incubated at 37 $^{\circ}$ C for 24 h. The oxidation reaction was terminated by the addition of butylated hydroxytoluene (BHT) in ethanol (50 μ l of 2 mM in ethanol to give 40 μ M final concentration) and catalase (125 μ l of 1.5 mg/ml in water, to give 300 nM final concentration) to the reaction mixture, and then extracted immediately by the Bligh & Dyer method [33]. After evaporation of solvent under a stream of dry argon, the residue was subjected to PLA₂-catalyzed hydrolysis. Thus, the extract was dissolved in methanol (50 μ l). Then 450 μ l of PBS solution (10mM, pH 7.4) and 50 μ l of CaCl₂ (50mM) were added. The resulting mixture was sonicated for 10 min followed by the addition of 50 μ l of PLA₂ (10,000 unit/ml). After incubation at 37 $^{\circ}$ C for 10 h under argon, the resulting mixture was extracted three times with 750 μ l of methanol/chloroform (1:2, v/v). Solvents were evaporated under a stream of argon and stored in vials sealed under argon at -80 $^{\circ}$ C before being analyzed using LC-MS/MS.

Extraction of plasma lipids

Plasma samples were extracted by a modified Bligh & Dyer method adapted for small-scale with precautions (addition of BHT and EDTA) to prevent *in vitro* oxidation. In brief, plasma (200 μ l) was mixed with 750 μ l of chloroform/ methanol (1:2, v/v) containing 1 mM BHT. For LC/MS analysis, 2 or 2.6 ng of internal standard (iso[4]LGE₂-D31-lysoPE-HL) was included in this solution. The resulting mixture was vortexed for 15 min to maximize the extraction efficiency. Chloroform (250 μ l) was added and the mixture was vortexed for 1 min. Then aqueous sodium chloride (250 μ l of 1.5%) was added and the mixture was vortexed for 1 min. The resulting mixture was centrifuged (3000 rpm) for 10 min to give a three-phase system (aqueous top, protein disk, organic bottom). The bottom layer was carefully withdrawn with a polyethylene transfer pipette (Fisher catalogue number 13-711-31), making sure to avoid the interface or upper layer. The solvents were then evaporated under a stream of argon at room temperature, and the sample was stored under argon at -80 $^{\circ}$ C before being analyzed using LC-MS/MS.

Extraction of tissue lipids

Liver samples from chronic ethanol-fed mice (C57BL/6 female) and control mice, pair-fed diets which iso-calorically substituted maltose dextrins for ethanol, were prepared as described

in a companion paper [34]. The liver tissue was extracted by the Folch method [35]. Tissue was placed in a tube with chloroform/methanol (2:1, v/v) containing 1 mM BHT and 10 ng/ml of internal standard iso[4]LGE₂-D31-lysoPE-HL (2 ml of Folch solution per 100 mg of tissue). The tissue was homogenized manually using a Teflon-coated stainless steel pestle. After homogenization, the resulting mixture was placed in a 4 °C freezer for 30 min to maximize extraction efficiency of lipids. An aqueous solution of sodium chloride (1.5%, w/w, 1/4 the volume of the organic extract) was added. The resulting mixture was centrifuged at 3000 rpm for 15 min. The lower layer containing the lipids was carefully withdrawn with a polyethylene transfer pipette, making sure to avoid the interface or upper layer. The solvents were then evaporated under a stream of dry argon at room temperature, and the sample was stored under argon at -80 °C before being analyzed using LC-MS/MS.

PLA₂ catalyzed hydrolysis of esterified isoLG-lysoPE adducts from biological samples

Time course of the PLA₂-catalyzed hydrolysis of the lipid extract from a plasma sample—The total lipid extract from 2 ml of plasma was dissolved in methanol (500 µl) followed by the addition of PBS solution (5 ml of 10 mM, pH 7.4) containing CaCl₂ (5 mM). The resulting mixture was sonicated for 5 min followed by the addition of PLA₂ (500 µl of 10,000 units/ml). The resulting mixture was incubated under argon at 37 °C. Aliquots (600 µl) were withdrawn at various times and extracted immediately by the method of Bligh & Dyer (see “*extraction of plasma lipids*”, above), solvent was evaporated under a stream of dry argon and the lipids were stored in vials under argon at -80 °C until LC-MS/MS analysis.

Processing of biological phospholipid extracts—The total lipid extract from biological samples (200 µl of plasma or 100 mg of tissue) was dissolved in methanol (50 µl) followed by the addition of a PBS solution (10 mM, pH 7.4, 450 µl) containing CaCl₂ (5 mM). The resulting mixture was sonicated for 5 min followed by the addition of PLA₂ enzyme (50 µl of 10,000 units/ml). The resulting mixture was incubated under argon at 37 °C. Aliquots (200 µl) were withdrawn at various times and extracted immediately by the Bligh & Dyer method (see “*extraction of plasma lipids*”, above) and stored in vials under argon at -80 °C prior to LC-MS/MS analysis.

Overall recovery after the sample pretreatment steps

To assess recovery of iso[4]LGE₂-lysoPE-HL from plasma, pure synthetic iso[4]LGE₂-lysoPE-HL (10 µl of 0.2 µg/ml in methanol) was added to plasma (200 µl). Then the mixture was extracted by the Bligh & Dyer method as described for extraction of plasma total lipids. The extract was dissolved in 50 µl of methanol followed by the addition of 450 µl of PBS solution (10 mM, pH 7.4). The resulting mixture was sonicated for 5 min. Note that the addition of PLA₂ and CaCl₂ was omitted to avoid generation of additional iso[4]LGE₂-lysoPE-HL from endogenous phospholipids in the plasma. The resulting mixture was then extracted again by the Bligh & Dyer method. After evaporation of solvents under a stream of dry argon, the final extract was dissolved in methanol (200 µl) containing iso[4]LGE₂-D31-lysoPE-HL (2 ng as internal standard). The resulting mixture (20 µl) was quantitated by LC-MS/MS. Pure synthetic iso[4]LGE₂-lysoPE-HL (10 µl of 0.2 µg/ml in methanol) was added to 200 µl of methanol containing iso[4]LGE₂-D31-lysoPE-HL (2 ng as internal standard). The resulting mixture (20 µl) was quantitated by LC-MS/MS. Recovery was determined by the ratio of iso[4]LGE₂-lysoPE-HL concentration after sample pretreatment to that without extraction.

Derivatization of synthetic or endogenous isoLG-lyso-PE-HL

Pentafluorobenzyl (PFB) ester derivatives of lipids were prepared by suspending the synthetic isoLG-lyso-PE-HL (40 µg) or lipid extract from human plasma (200 µl) in anhydrous acetonitrile containing 10% pentafluorobenzyl bromide (PFB-Br) and 20% N,N-

diisopropylethylamine (500 μ l) at room temperature for 1 h. Solvent and volatile reagents were then evaporated under a stream of argon. Nonlipid components were removed by solid-phase extraction: the product mixture was transferred with 50% methanol in water (2×1 ml) and loaded on C18 minicolumn (Strata C18-T solid phase extraction tubes, 6 ml, Phenomenex, Torrance, CA). Nonlipid components were then removed by eluting with 75% methanol in water (6 ml). The lipid derivatives were then eluted with methanol (2 ml), and the solvents were evaporated under a stream of dry argon.

Mass spectrometry

Direct infusion MS and LC-MS/MS were performed on a Quattro Ultima triple-quadrupole mass spectrometer (Micromass, Wythenshawe, UK). The tuning parameters of mass spectrometer were optimized for each MS/MS transition by utilization of synthetic standards. The total ion current was measured in the mass range of m/z 50–900 at 30 V of cone energy in the negative ion mode with a 3.5 kV electrospray capillary voltage, 60 V cone voltage, 120 $^{\circ}$ C source temperature, 250 $^{\circ}$ C desolvation temperature, 65 L/h cone gas flow and 658 L/h desolvation gas flow. A parent-to-daughter ion transition of m/z 800.2 \rightarrow 153 was monitored for iso[4]LG-lysoPE-HLs (collision energy 45 eV), 784.2 \rightarrow 153 for iso[4]LG-lysoPE-lactam (collision energy 55 eV), 768.2 \rightarrow 153 for iso[4]LG-lysoPE-pyrrole (collision energy 50 eV) and 831.2 \rightarrow 153 for iso[4]LGE₂-D31-lysoPE-HL internal standard (collision energy 40 eV) as quantifier for the multiple reaction monitoring (MRM) with a dwell time of 200 ms. Chromatographic separation was achieved using a Luna C18 column (150 \times 2.0 mm i.d., 5 μ m particle size, Phenomenex) connected to a Waters Alliance 2690 (Waters, Wilmington, DE) HPLC system (pump and autosampler) for injection of the samples. Samples were eluted with a binary solvent gradient (methanol as solvent A and water as solvent B, with both mobile phases supplemented with 2 mM ammonium acetate to enhance the MS signal). A linear gradient was run from 75% to 100% solvent A over 10 min. After holding this solvent composition for 7 min, the mobile phase was linearly changed back to the initial mobile phase composition (75% methanol in water) over 0.5 min, and the column was equilibrated under this condition for 7.5 min prior to the next injection. A flow rate of 0.2 ml/min and a run time of 25 min were used for all analyses. All retention times of analytes shown in MRM spectra were recorded relative to internal standard (iso[4]LGE₂-D31-lysoPE-HL, 11.83 min). Lipid extracts from biological matrices were reconstituted with methanol (200 μ l). An aliquot (20 μ l) of the solution was employed for each LC-MS/MS analysis. We chose 800.2 \rightarrow 153.0, the transition with strongest intensity, for quantitation of isoLG-PE-HLs in biological matrices. The concentration of the isoLG-lysoPE-HLs in samples was determined by interpolation from the peak area ratio of iso[4]LGE₂-D31-lysoPE-HL versus isoLG-lysoPE-HLs using a standard curve for iso[4]LGE₂-lysoPE-HL as described above. MS/MS data analyses were performed with Masslynx software (version 3.5, Waters Micromass).

Statistics

The data represent the means \pm S.D. of the indicated numbers of samples. The statistical analyses were made using a Student *t*-test (two-sample assuming equal variances). For all of these hypotheses, the significance level was 0.05.

Results and Discussion

Mass spectrometric characterization of covalent adducts of iso[4]LGE₂ with 2-lysoPE

Pyrrole (M.W. 769), lactam (M.W. 785) and hydroxylactam adducts (M.W. 801) generated in the reaction of iso[4]LGE₂ with 2-lysoPE were analyzed by direct infusion MS in the negative ion mode. Representative collision-induced dissociation (CID) spectra of the three adducts are shown in Fig. 2. The CID fragments with mass-to-charge ratio (m/z) 79, 153, 255 and 512 (Fig. 2A and supplementary material Fig. S5) are preceded (supplementary material S6) [26].

The structure of the fragment ion with m/z 409 is deduced by analogy with a fragmentation mechanism suggested previously [26]. The structures of daughter ions at m/z 528 (Fig. 2B) and 544 (Fig. 2C) are deduced by analogy to the daughter ion at m/z 512. The daughter ions at m/z 388, 644 (Fig. 2B) and 404, 660 (Fig. 2C) are deduced by analogy with a fragmentation mechanism suggested previously (supplementary material S5 and S6) [36–38].

The fragments with m/z 79, 153, 255 and 409 in the pyrrole (Fig. 2A), lactam (Fig. 2B) and hydroxylactam (Fig. 2C) all correspond to isoLG-lysoPE adducts but do not distinguish isoLG structural isomers. The ion at m/z 79 indicates the formation of the phosphate-derived ion. The daughter ion at m/z 153 represents the combined losses of the palmitic acid and the isoLG-ethanolamine moiety. An ion at m/z 255 represents a palmitate anion from the *sn*-1 position. A fragment ion at m/z 409 corresponds to neutral loss of the isoLG-ethanolamine moiety. Daughter ions at m/z 512, 528 and 544 correspond to loss of the *sn*-1 palmitoyl moiety from pyrrole, lactam and hydroxylactam adducts, respectively (Fig. 2 and supplementary material Fig. S1). The daughter ions at m/z 388 and 644 are *unique for lysoPE-lactam adducts of iso[4]LGE₂* (Fig. 2B), while *the daughter ions at m/z 404 and 660 are unique for the lysoPE-HL adduct of iso[4]LGE₂* (Fig. 2C and supplementary material Fig. S7). Diagnostic daughter ions with side-chain isomer specific structural information, e.g., at m/z 372 and 628, which represent the side-chain fragment from iso[4]LGE₂-lysoPE-pyrrole were not observed in the CID MS of the pyrrole adduct.

The pure hydroxylactam, isoLG-lysoPE-HL, was isolated by preparative HPLC from the mixture of adducts generated in the reaction of iso[4]LGE₂ with lysoPE. The hydroxylactam was further characterized by NMR (Fig. 1 and S2). For the quantification of level of isoLG adducts of lyso-PE generated *in vitro* or *in vivo*, we synthesized an isotope labeled hydroxylactam adduct, iso[4]LGE₂-D31-lysoPE-HL, that was also characterized by NMR and LC-MS/MS (spectra are presented in Fig. S3 and S4).

The above results provided an LC-MS/MS method to simultaneously identify and quantify individual iso[4]LGE₂-lysoPE adducts. Pyrrole adducts were detected by multiple reaction monitoring (MRM) of the transitions between 5 daughter ions common to all isoLG structural isomers and the parent ions at m/z 768. Lactam and hydroxylactam adducts of iso[4]LGE₂ and lysoPE were detected by MRM of the transitions between the parent ions from lactam and hydroxylactam adducts, respectively, and 5 daughter ions common to all isoLG structural isomers as well as 2 daughter ions diagnostic of the unique side chains of iso[4]LG structural isomers (Fig. 3).

Time course for the formation of covalent adducts of iso[4]LGE₂ with 2-lysoPE

The results of a study of the time course of the reaction between iso[4]LGE₂ and lysoPE are shown in Fig. 4. Initially the yield of the pyrrole climbs, but then drops after 2 h as expected for an intermediate in the production of the lactam and hydroxylactam adducts. After incubation for 36 h, the hydroxylactam (iso[4]LGE₂-lysoPE, 36%) and lactam (26%) are the major covalent adducts of iso[4]LGE₂ with lyso-PE. The final yield of pyrrole adduct is very low because of its proclivity to autoxidation to give lactams and hydroxylactams.

Formation of isoLG-lysoPE-lactams and isoLG-lysoPE-hydroxylactams during MPO catalyzed oxidation of PA-PC in the presence of lysoPE

The LC-MS/MS method described above was used to show that isoLG-lysoPE adducts can be generated *in vitro* using a well-defined and biologically relevant model system for lipid oxidation. We exposed PA-PC to the MPO/glucose(G)-glucose oxidase/NO₂- oxidation system in the presence of lysoPE and examined the reaction mixture for the presence of isoLG-lysoPE adduct. As shown in Fig. 5, the MPO catalyzed oxidation of PA-PC in the presence of

lysoPE, followed by PLA₂-catalyzed hydrolysis, generated both isoLG-lysoPE-lactam and isoLG-lysoPE-HL adducts that demonstrated the same retention times for the selected transitions between parent and daughter ions as the authentic standard iso[4]LG-lysoPE-lactam and iso[4]LG-lysoPE-HL adducts shown in Figure 3.

A careful inspection of the data in figure 3 and figure 5 reveals considerable variations in the ratios of major chromatographic peaks. For example for the isoLG-lysoPE-HL, relative to the 800>153 transition, the 800>79 transition is 15% in Figure 3C and 66% in figure 5B and the 800>255 transition is 50% in figure 3C and 37% in figure 5B. By implementing the isotope dilution technique, a major improvement in precision was achieved. For example for the isoLG-lysoPE-HL after internal standard correction, relative to the 800>153 transition, the 800>79 transition is 15% in Figure 3C and 14% in figure 5B and the 800>255 transition is 50% in figure 3C and 48% in figure 5B (see supplementary tables S1–S3). This supports the conclusion that the imprecision of the uncorrected peak ratios is caused by variations from one LC-MS/MS run to another in collision energy, cone voltage or other factors that change ionization efficiency (parent ions) or fragmentation efficiency (daughter ions) rather than, e.g., a consequence of interfering compound(s) present in the MPO-derived sample. The isotope dilution technique contributes significantly to the precision of the quantitative analysis of isoLG-lysoPE-HLs by LC-MS/MS.

Collectively, these results indicated that isoLGs generated from free radical-induced oxidation of arachidonate-containing phospholipids covalently bind phosphatidylethanolamine species *in vitro* and led to the expectation that these adducts are formed *in vivo*.

Initially no isoLG-lysoPE adducts were detected in lipid extracts from human plasma

For detecting their presence *in vivo*, we initially examined whether or not isoLG-lysoPE-lactam and isoLG-lysoPE-HL adducts could be detected in the total lipid extract from human plasma samples from healthy individuals. We could not find the peaks in the MRM transitions representing lactam and hydroxylactam adducts (supplementary figure S8). Furthermore, none of the MRM channels anticipated for isoLG-modified dP-PE, PO-PE, PL-PE, PA-PE or PD-PE species provided any detectable signal (Data not shown). We reasoned that lack of detection of isoLG-phospholipid adducts under the initial conditions might be a consequence of their presence as a complex mixture of homologs containing a large variety of different acyl groups esterified to the *sn*-2 hydroxyl group, none of which is present in adequate concentrations to provide a detectable signal.

Detection of isoLGs-lysoPE-HLs in lipid extracts from human plasma after PLA₂ treatment

Although the isoLG moiety of the expected adducts are anticipated to be comprised of eight structural isomers, this isomerism will not interfere with the MS analysis because all of these isomers have the same molecular weight and are expected to have similar HPLC elution times. Furthermore, in the glycerophosphoethanolamine moiety, the *sn*-1 position is usually bound with saturated acyl groups, predominately palmitic acid (16:0) and lesser amounts of stearic acid (18:0). However, the *sn*-2 position may be esterified with a variety of saturated or unsaturated fatty acyls [39]. This variance in *sn*-2 acyl groups of glycerophospholipid moieties affords a complex mixture of isoLG-modified PEs with different molecular weights in which the amount of each species could be lower than the lowest limit of mass spectrometric detection. To overcome this problem, we converted the putative complex mixture of isoLG-modified PEs into a much simpler mixture by phospholipase A₂ (PLA₂)-catalyzed selective hydrolysis of the *sn*-2 acyl, releasing 2-lysophospholipids [40]. To prevent *in vitro* oxidation, the presence of a transition metal ion chelator (EDTA) was essential at all stages of sample processing. Even in the presence of an excess of Ca⁺², required by the enzyme PLA₂, EDTA remains an effective chelator of transition metal ions because the stability constants for their EDTA complexes,

e.g., $\log K = 18.8$ or 25.1 for Cu^{+2} or Fe^{+3} , are much greater than that of Ca^{+2} , i.e., $\log K = 10.7$ [41].

Analysis of a lipid extract from plasma treated with PLA_2 revealed the presence of isoLG-lysoPE-HL but not isoLG-lysoPE-lactam (data not shown) confirming that isoLG-PE-HLs are present *in vivo*. As shown in Fig. 6, the MRM transitions corresponding to all isoLG-lysoPE-HL adducts co-eluted at a single retention time identical with that of the pure synthetic iso[4]LGE₂-lysoPE-HL standard. However, the transitions corresponding to structurally unique fragmentations that are diagnostic for iso[4]LGE₂-lysoPE-HL were not detectable. By comparison between behaviors of putative isoLG-lysoPE-HL and the synthetic standard of iso[4]LGE₂-lysoPE-HL in biological matrices, we noticed the absence of diagnostic transitions m/z 800.2→403.9 and 800.2→660.2 corresponding to iso[4]LGE₂-lysoPE-HL, as well as the interference from components in the biological sample (matrix effect) in the transition m/z 800.2→255.2 common to all isoLG-lyso-PE-HLs (supplementary figure S9). Although they could be detected in the mixture of adducts generated from oxidation of PA-PC in the presence of 2-lyso-PE (Figure 5B) followed by selective hydrolysis with PLA_2 , neither they nor those expected from the regioisomeric isoLG-lysoPE hydroxylactams (supplementary figure S7) could be detected in the mixture of adducts derived from human plasma. These limitations are probably a consequence of the fact that the amount of iso[4]LGE₂-lysoPE-HL is only a small portion in the total of all isoLG-lysoPE-HL structural isomers present *in vivo*. Furthermore, the fragmentation efficiency of the diagnostic transitions for iso[4]LGE₂-lysoPE-HL could be suppressed by a matrix effect of components in plasma samples.

Because small retention time differences are apparent between the peaks attributed to isoLG-lysoPE-HLs in Fig. 6A and 6B, we performed a control experiment to confirm that the compounds detected in the plasma sample of 6A are isoLG-lysoPE-HLs. Thus, a sample of plasma extract, after PLA_2 treatment, was spiked with authentic standard iso[4]LGE₂-lysoPE-HL. As shown in figure 7, only a single peak was detected in the lipid extract after PLA_2 treatment to which was added approximately the same amount of authentic standard (0.5 ng) as there was isoLG-lysoPE-HL presumed to be present in the samples shown in panel A. Although the total ion current of each scan in panel B is approximately double that in panel A, only a single peak is seen in each scan.

To further confirm the identity of these *in vivo*-derived compounds as isoLG-lysoPE-HLs, the lipid extracts from biological samples were treated with a mixture of pentafluorobenzyl bromide (PFB-Br) and diisopropylethylamine to derivatize the carboxylic acid functionality. This introduces a net increase of 180 Da in the molecular weight. The PFB derivative of pure iso[4]LGE₂-lysoPE-HLs obtained by chemical synthesis was also prepared as an authentic standard. As shown in Fig. 8, before PFB esterification, no peaks were seen in the MRM transition m/z 980.2→153.0. A peak with the same retention time as the synthetic PFB ester of iso[4]LGE₂-lysoPE-HL appears in the channel 980.2→153.0 after esterification. This further confirmed the presence of HL adducts of isoLG-modified PEs *in vivo*. Furthermore, the peak in MRM transition m/z 800.2→153.0, which represents isoLG-lysoPE-HLs, disappears after esterification (Fig. 8B). Both of these results further confirmed that HL adducts of isoLG-modified PEs are present *in vivo*.

A calibration curve for iso[4]LGE₂-lysoPE-HL was constructed in blank plasma without PLA_2 treatment (Fig 9). We also constructed calibration curves for iso[4]LGE₂-lysoPE-HL in blank plasma with PLA_2 treatment and in PBS buffer (Fig. 9). The three graphs are parallel straight lines. This supports the view that the isotope labeled internal standard efficiently minimizes any matrix effect for the biological samples. Moreover, the non zero y-intercept of the calibration constructed for blank plasma with PLA_2 treatment confirms the presence of

endogenous isoLG-PE-HL in plasma that becomes isoLG-lysoPE-HL upon treatment with PLA₂.

Subsequently, we optimized the time for PLA₂-catalyzed hydrolysis of plasma lipid extracts. Fig. 10 shows the evolution profiles and maximum and final level for isoLG-lysoPE-HL produced upon PLA₂ hydrolysis of a lipid extract. The level of isoLG-lysoPE-HL in the sample reaches a maximum (plateau) after incubation for 10 h at 37 °C.

Replicate analyses of different plasma samples (n = 5, Table 1) as well as plasma samples spiked with known amounts of pure iso[4]LGE₂-lysoPE-HLs (Table 2) were conducted. The results show that our quantitative method has excellent precision and accuracy.

In theory, two compounds that are isobaric with 2-lysoPE, i.e., the ether lipid C17:0e/C18:0-glyeroPE or the plasmalogen C17:0p:C16:0-glycerPE, could interfere with our assay. However, the vast majority of natural fatty acids have an even number of carbon atoms because their biosynthesis involves oligomerization of the two-carbon synthon acetyl-CoA. Alkyl or alkenyl chains with 17 carbons are not major constituents of natural lipids, and such C17 phosphatidylethanolamine derivatives are rare *in vivo*. It is highly unlikely that such putative naturally occurring isobaric compounds interfere with the assay of isoLG-lysoPE-HLs.

IsoLG-lysoPE-HLs can provide a sensitive LC-MS/MS marker of oxidative injury

Our previous studies showed that iso[4]LG-protein adduct levels provide a unique dosimeter of oxidative injury. We previously reported that plasma levels of isoLG-protein adducts are significantly elevated in patients with atherosclerosis or end-stage renal disease compared to normal individuals [13,15]. We found significant elevations in the levels of these markers of oxidative injury in patients with cardiovascular disease who had undergone coronary artery bypass surgery. Especially noteworthy was the observation that levels of cholesterol in these patients were significantly lower than those in younger healthy individuals. Presumably dietary or medicinal interventions were successfully lowering levels of cholesterol in the cardiovascular disease patients, but levels of oxidative injury, perhaps an indication of chronic inflammation, remained high. Since elevated oxidative injury in these patients may have pathological significance, a sensitive and efficient method is needed to monitor the efficacy of therapeutic interventions. Unfortunately, MS methodology for measuring protein-bound LGs/isoLGs requires large sample sizes, e.g. 2 ml of plasma, and time-consuming sample preparation to excise LG/isoLG-modified lysine from proteins [42]. Especially notable are the facts that (1) the LG/isoLG-PE-HLs are detectable in biological samples that are an order of magnitude smaller and (2) sample processing is much simpler and less time-consuming than required for detecting the corresponding LG/isoLG-lysyl-lactams [42]. Both features enhance the potential clinical utility of LG/isoLG-PE-HLs compared to the protein-derived lysyl-lactam analogues.

Liver isoLG-PE-HL adduct levels are elevated in chronic ethanol-fed mice

Mounting evidence over the past decade indicates that reactive oxygen species (ROS) play a critical role in ethanol-induced liver injury [43,44]. ROS can also induce cyclo-oxygenation of polyunsaturated fatty acids to form various γ -ketoaldehydes, including LGE₂ and iso[4] LGE₂ [14,15,45]. We hypothesized that ethanol exposure induces formation of LG/isoLGs, that subsequently modify phosphatidylethanolamines resulting in increased levels of isoLG-PE-HL in the liver of a murine model of alcoholic liver disease.

In an *in vivo* study, we compared the levels of isoLG-lysoPE-HL adducts in livers from chronic ethanol (27% of calories for 4 weeks)-fed mice (n = 6) with control animals (n = 4, pair-fed diets which iso-calorically substituted maltose dextrins for ethanol) by liquid chromatography-

tandem mass spectrometry (LC-MS/MS) after selective phospholipolysis with PLA₂ (Fig. 11). Two-fold higher levels ($P = 0.00021$) were detected in livers from chronic ethanol-fed mice (32.4 ± 6.3 ng/g) compared to pair-fed mice (12.1 ± 1.5 ng/g). Our results confirmed that ethanol exposure enhanced the formation of isoLGs and the derived isoLG-PE-HLs in mouse liver.

Plasma isoLG-lysoPE-HL levels are elevated in age-related macular degeneration

There is growing consensus that age-related macular degeneration is an age-related inflammatory disease triggered in part by oxidative stress. A host of oxidative protein and DNA modifications have been detected at elevated levels in human age-related macular degeneration tissues, including in plasma carboxyethylpyrrole (CEP), an oxidative protein modification generated from docosahexaenoate-containing phospholipids [30,46], and carboxymethyllysine and pentosidine, oxidative protein modifications generated from sugars through the Maillard reaction [47]. We hypothesized that chronic inflammation in age-related macular degeneration patients would result in elevated plasma levels of isoLG-PE adducts. In a pilot clinical study, we compared isoLG-lysoPE-HL levels in plasma from age-related macular degeneration and age and gender matched control subjects (Fig. 12). The mean level detected in age-related macular degeneration plasma (5.2 ± 0.4 ng/ml, $n = 15$ patients) was significantly elevated ($P < 0.0001$) compared with plasma from healthy volunteers (3.4 ± 0.1 ng/ml, $n = 15$). Our preliminary results support the potential utility of these ethanolamine phospholipid adducts as biomarkers for detecting risk to diseases stimulated by oxidative stress. The results also reinforce the association between oxidative stress and age-related macular degeneration and are consistent with the hypothesis that age-related macular degeneration is a systemic disease [47–49]. A much larger clinical study is now warranted, including evaluation of the possibility that isoLG-lysoPE-HL plasma levels in combination with other biomarkers, may enhance prognostic utility. For example, we recently demonstrated that for individuals exhibiting elevated carboxyethylpyrrole marker levels, the risk for age-related macular degeneration was increased ~2-3-fold relative to that predicted by age-related macular degeneration risk genotype alone [29]. This study showed that combined carboxyethylpyrrole proteomic and genomic biomarker measurements are more effective in predicting age-related macular degeneration risk than either method alone [29]. Other recent proteomic studies suggest that plasma protein levels of CML together with pentosidine discriminate between age-related macular degeneration and control patients with 89% accuracy and that pentosidine in combination with carboxyethylpyrrole adducts can discriminate with 92% accuracy [47]. Thus, isoLG-lysoPE-HL measurements in combination with other biomarkers, may improve methods for disease prognosis and for monitoring therapeutic efficacy.

Biological Significance of PE modification by LGs or isoLGs

Oxidatively damaged LDL accumulates in atherosclerotic plaques owing to endocytosis by monocyte macrophages in the subendothelial space. Because ethanolamine phospholipids constitute only a few percent of total LDL phospholipids [50], their physiological roles may be especially susceptible to interference by covalent modification which may also generate pathological new activities. The accumulation of aldehyde-modified PEs in atherosclerotic lesions but not in circulating LDL suggests an atherogenic role [51]. Covalent modification of the primary amino group in LDL PEs by aldehydes was postulated to contribute to prothrombotic activity involving stimulation of platelet prothrombinase activity [52].

Besides their potential as clinically useful dosimeters of oxidative injury, the present demonstration of the presence of LG/isoLG-modified ethanolamine phospholipids *in vivo* may have pathological significance arising from the effects of these modifications on membrane function. Ethanolamine phospholipids account for 27 – 52% of total phospholipids in brain (52% in myelin white matter), heart, liver, kidney, spleen, erythrocytes, and platelets [53]. Since PE prefers to organize itself into non-bilayer structures, it is noteworthy that

biomembranes contain a substantial amount of this non-bilayer lipid. The fact that levels of non-bilayer lipids are precisely regulated implies “that they are of considerable functional importance” [54]. Apparently, the biological activity of some membrane proteins, such as transporters, depend on the presence of PE, since its depletion causes a loss of activity which is restored upon replacing the PE [54]. Therefore, modifications of ethanolamine phospholipids by covalent adduction of their primary amino residues with lipid oxidation products could compromise membrane function, e.g., by impairing their ability to stabilize membrane proteins. Membrane structure and the interaction of membrane PEs with membrane-bound or cytosolic proteins may be profoundly altered by the conversion of the positively charged amino group of the PEs into a negatively charged group upon conversion to LG/isoLG-PE-HL derivatives. Modifications of ethanolamine phospholipids may be of mechanistic significance for the loss of blood-brain barrier integrity that we detected as a consequence of injecting minute quantities of LGE₂ into rat brain [55].

Mitochondrial membrane is especially vulnerable to oxidative damage because various free radical species are generated by components of the electron transport chain in the membrane during mitochondrial respiration. Modification of PE by lipid oxidation products, such as HNE, was proposed to account for the formation of fluorescent chromolipids upon oxidation of rat liver microsomes or mitochondria [56], and covalent modification by lipid peroxidation products was shown to alter membrane fluidity [57]. The possible contribution of LGs/isoLGs to the production of such chromolipids merits investigation.

Reaction of LGs/isoLGs with proteins generates protein-protein crosslinks orders of magnitude more rapidly than other products of lipid oxidation, e.g., MDA [58]. Interestingly, MDA accumulation disturbs the organization of ethanolamine phospholipids in the human erythrocyte membrane, and it was suggested that this might be a consequence of cross linking by MDA [59]. Covalent adduction of LGs or isoLGs with PEs is not only expected to cause PE-PE cross linking in analogy with their ability to generate protein-protein cross links, but also could crosslink proteins with phospholipids resulting in anchoring of proteins to membranes.

Supplementary Material

Refer to Web version on PubMed Central for supplementary material.

Acknowledgments

This work was supported by NIH grants AA013868 and AA011975 to LE Nagy; GM021249 and HL087018 to RG Salomon; and EY014239 to JW Crabb; and BRTT grant 05–29 from the State of Ohio to JW Crabb and RG Salomon.

Abbreviations

BHT, butylated hydroxytoluene
¹³C NMR, carbon magnetic resonance
CDCl₃, deuterated chloroform
CID, collision-induced dissociation
D62-dP-PE, 1,2-dipalmitoyl-d₆₂-sn-glycero-3-phosphoethanolamine
dP-PE, 1,2-dipalmitoyl-sn-glycero-3-phosphoethanolamine
DTPA, diethylenetriamine pentaacetic acid
ESI, electrospray ionization
HNE, 4-hydroxy-2-nonenal
¹H NMR, proton magnetic resonance
HPLC, high-performance liquid chromatography
isoLG, isolevuglandin

iso[4]LGE₂, iso[4]levuglandin E₂
 iso[4]LGE₂-D31-lysoPE-HL, iso[4]levuglandin E₂-d₃₁-lyso-phosphatidylethanolamine-hydroxylactam
 iso[7]LGD₂, iso[7]levuglandin D₂
 LC-MS/MS, liquid chromatography/tandem mass spectrometry
 LDL, low density lipoprotein
 LG, levuglandin
 lysoPE, 1-palmitoyl-2-hydroxyl-*sn*-glycero-3-phosphatidylethanolamine
 MDA, malondialdehyde
 MPO, myeloperoxidase
 MRM, multiple reaction monitoring
 MS, mass spectrometry
 PA-PC, 1-palmitoyl-2-arachidonoyl-*sn*-glycero-3-phosphatidylcholine
 PA-PE, 1-palmitoyl-2-arachidonoyl-*sn*-glycero-3-phosphatidylethanolamine
 PE, phosphatidylethanolamine
 PD-PE, 1-palmitoyl-2-docosahexanoyl-*sn*-glycero-3-phosphatidylethanolamine
 PL-PE, 1-palmitoyl-2-linoleoyl-*sn*-glycero-3-phosphatidylethanolamine
 PO-PE, 1-palmitoyl-2-oleyl-*sn*-glycero-3-phosphatidylethanolamine
 PBS, phosphate buffered saline
 PFB-Br, pentafluorobenzyl bromide
 PLA₂, phospholipase A₂
 ROS, reactive oxygen species

References

- Salomon RG, Miller DB, Zagorski MG, Coughlin DJ. Solvent Induced Fragmentation of Prostaglandin Endoperoxides. New Aldehyde Products from PGH₂ and a Novel Intramolecular 1,2-Hydride Shift During Endoperoxide Fragmentation in Aqueous Solution. *J Amer Chem Soc* 1984;106:6049–6060.
- Salomon RG, Miller DB. Levuglandins: isolation, characterization, and total synthesis of new secoprostanoic products from prostaglandin endoperoxides. *Adv Prostaglandin Thromboxane Leukot Res* 1985;15:323–326. [PubMed: 2936114]
- Salomon RG, Subbanagounder G, Singh U, O'Neil J, Hoff HF. Oxidation of low-density lipoproteins produces levuglandin-protein adducts. *Chem Res Toxicol* 1997;10:750–759. [PubMed: 9250408]
- Brame CJ, Salomon RG, Morrow JD, Roberts LJ 2nd. Identification of extremely reactive gamma-ketoaldehydes (isolevuglandins) as products of the isoprostane pathway and characterization of their lysyl protein adducts. *The Journal of biological chemistry* 1999;274:13139–13146. [PubMed: 10224068]
- Salomon RG. Distinguishing levuglandins produced through the cyclooxygenase and isoprostane pathways. *Chem Phys Lipids* 2005;134:1–20. [PubMed: 15752459]
- Bernoud-Hubac N, Davies SS, Boutaud O, Montine TJ, Roberts LJ 2nd. Formation of highly reactive gamma-ketoaldehydes (neuroketals) as products of the neuroprostane pathway. *The Journal of biological chemistry* 2001;276:30964–30970. [PubMed: 11413140]
- Salomon RG, Jirousek MR, Ghosh S, Sharma RB. Prostaglandin endoperoxides 21. Covalent binding of levuglandin E₂ with proteins. *Prostaglandins* 1987;34:643–656. [PubMed: 3481092]
- Boutaud O, Brame CJ, Salomon RG, Roberts LJ 2nd, Oates JA. Characterization of the lysyl adducts formed from prostaglandin H₂ via the levuglandin pathway. *Biochemistry* 1999;38:9389–9396. [PubMed: 10413514]
- Amarnath V, Valentine WM, Amarnath K, Eng MA, Graham DG. The mechanism of nucleophilic substitution of alkylpyrroles in the presence of oxygen. *Chem Res Toxicol* 1994;7:56–61. [PubMed: 8155825]
- Roberts LJ 2nd, Salomon RG, Morrow JD, Brame CJ. New developments in the isoprostane pathway: identification of novel highly reactive gamma-ketoaldehydes (isolevuglandins) and characterization of their protein adducts. *Faseb J* 1999;13:1157–1168. [PubMed: 10385607]

11. Kobierski ME, S K, Murthi KK, Iyer RS, G SR. Synthesis of a Pyrazole Isostere of Pyrroles formed by the Reaction of the ϵ -Amino Groups of Protein Lysyl Residues with Levuglandin E₂. *J Org Chem* 1994;59:6044–6050.
12. Salomon RG, Sha W, Brame C, Kaur K, Subbanagounder G, O'Neil J, Hoff HF, Roberts LJ 2nd. Protein adducts of iso[4]levuglandin E₂, a product of the isoprostane pathway, in oxidized low density lipoprotein. *The Journal of biological chemistry* 1999;274:20271–20280. [PubMed: 10400646]
13. Poliakov E, Meer SG, Roy SC, Mesaros C, Salomon RG. Iso[7]LGD₂-protein adducts are abundant in vivo and free radical-induced oxidation of an arachidonyl phospholipid generates this D series isolevuglandin in vitro. *Chem Res Toxicol* 2004;17:613–622. [PubMed: 15144218]
14. Salomon RG, Subbanagounder G, O'Neil J, Kaur K, Smith MA, Hoff HF, Perry G, Monnier VM. Levuglandin E₂-protein adducts in human plasma and vasculature. *Chem Res Toxicol* 1997;10:536–545. [PubMed: 9168251]
15. Salomon RG, Batyreva E, Kaur K, Sprecher DL, Schreiber MJ, Crabb JW, Penn MS, DiCorletoe AM, Hazen SL, Podrez EA. Isolevuglandin-protein adducts in humans: products of free radical-induced lipid oxidation through the isoprostane pathway. *Biochim Biophys Acta* 2000;1485:225–235. [PubMed: 10832102]
16. Brame CJ, Boutaud O, Davies SS, Yang T, Oates JA, Roden D, Roberts LJ 2nd. Modification of proteins by isoketal-containing oxidized phospholipids. *The Journal of biological chemistry* 2004;279:13447–13451. [PubMed: 14715668]
17. Salomon RG, Kaur K, Batyreva E. Isolevuglandin-protein adducts in oxidized low density lipoprotein and human plasma: a strong connection with cardiovascular disease. *Trends Cardiovasc Med* 2000;10:53–59. [PubMed: 11150730]
18. Evans TA, Siedlak SL, Lu L, Fu X, Wang Z, McGinnis WR, Fakhoury E, Castellani RJ, Hazen SL, Walsh WJ, Lewis AT, Salomon RG, Smith MA, Perry G, Zhu X. The Autistic Phenotype Exhibits a Remarkably Localized Modification of Brain Protein by Products of Free Radical-Induced Lipid Oxidation. *Am J Biotech Biochem* 2008;4:61–72.
19. Govindarajan B, Laird J, Salomon RG, Bhattacharya SK. Isolevuglandin-modified proteins, including elevated levels of inactive calpain-1, accumulate in glaucomatous trabecular meshwork. *Biochemistry* 2008;47:817–825. [PubMed: 18085799]
20. Salomon RG. Levuglandins and isolevuglandins: stealthy toxins of oxidative injury. *Antioxid Redox Signal* 2005;7:185–201. [PubMed: 15650407]
21. Salomon RG. Isolevuglandins, oxidatively truncated phospholipids, and atherosclerosis. *Ann N Y Acad Sci* 2005;1043:327–342. [PubMed: 16037255]
22. Murthi KK, Friedman LR, Oleinick NL, Salomon RG. Formation of DNA-protein cross-links in mammalian cells by levuglandin E₂. *Biochemistry* 1993;32:4090–4097. [PubMed: 8471616]
23. Murthi KK, Salomon RG, Sternlicht H. Levuglandin E₂ inhibits mitosis and microtubule assembly. *Prostaglandins* 1990;39:611–622. [PubMed: 2115185]
24. Guichardant M, Taibi-Tronche P, Fay LB, Lagarde M. Covalent modifications of aminophospholipids by 4-hydroxynonenal. *Free Radic Biol Med* 1998;25:1049–1056. [PubMed: 9870558]
25. Zemski Berry KA, Murphy RC. Characterization of acrolein-glycerophosphoethanolamine lipid adducts using electrospray mass spectrometry. *Chem Res Toxicol* 2007;20:1342–1351. [PubMed: 17636891]
26. Bernoud-Hubac N, Fay LB, Armarnath V, Guichardant M, Bacot S, Davies SS, Roberts LJ 2nd, Lagarde M. Covalent binding of isoketals to ethanolamine phospholipids. *Free Radic Biol Med* 2004;37:1604–1611. [PubMed: 15477011]
27. Poliakov E, Brennan ML, Macpherson J, Zhang R, Sha W, Narine L, Salomon RG, Hazen SL. Isolevuglandins, a novel class of isoprostenoid derivatives, function as integrated sensors of oxidant stress and are generated by myeloperoxidase in vivo. *Faseb J* 2003;17:2209–2220. [PubMed: 14656983]
28. Laird, JM. Chemistry. Cleveland: Case Western Reserve University; 2007. Isolevuglandin-derived hydroxylactams: Total synthesis and generation of an isoLG-modified lysine; p. 22–47.
29. Gu J, Paeur GJ, Yue X, Narendra U, Sturgill GM, Bena J, Gu X, Peachey NS, Salomon RG, Hagstrom SA, Crabb JW. Clinical Genomic And Proteomic Study, G. Assessing susceptibility to age-related

- macular degeneration with proteomic and genomic biomarkers. *Mol Cell Proteomics* 2009;8:1338–1349. [PubMed: 19202148]
30. Gu X, Meer SG, Miyagi M, Rayborn ME, Hollyfield JG, Crabb JW, Salomon RG. Carboxyethylpyrrole protein adducts and autoantibodies, biomarkers for age-related macular degeneration. *The Journal of biological chemistry* 2003;278:42027–42035. [PubMed: 12923198]
 31. Podrez EA, Poliakov E, Shen Z, Zhang R, Deng Y, Sun M, Finton PJ, Shan L, Febbraio M, Hajjar DP, Silverstein RL, Hoff HF, Salomon RG, Hazen SL. A novel family of atherogenic oxidized phospholipids promotes macrophage foam cell formation via the scavenger receptor CD36 and is enriched in atherosclerotic lesions. *The Journal of biological chemistry* 2002;277:38517–38523. [PubMed: 12145296]
 32. Podrez EA, Schmitt D, Hoff HF, Hazen SL. Myeloperoxidase-generated reactive nitrogen species convert LDL into an atherogenic form in vitro. *J Clin Invest* 1999;103:1547–1560. [PubMed: 10359564]
 33. Bligh EG, Dyer WJ. A rapid method of total lipid extraction and purification. *Can J Biochem Physiol* 1959;37:911–917. [PubMed: 13671378]
 34. Roychowdhury S, McMullen MR, Pritchard MT, Li W, Salomon RG, Nagy LE. Formation of γ -ketoaldehyde-protein adducts during early stages of ethanol induced liver injury. *Free Radic Biol Med*:submitted. 2009
 35. Folch J, Lees M, Sloane Stanley GH. A simple method for the isolation and purification of total lipides from animal tissues. *The Journal of biological chemistry* 1957;226:497–509. [PubMed: 13428781]
 36. Murphy RC, Barkley RM, Zemski Berry K, Hankin J, Harrison K, Johnson C, Krank J, McAnoy A, Uhlson C, Zarini S. Electrospray ionization and tandem mass spectrometry of eicosanoids. *Anal Biochem* 2005;346:1–42. [PubMed: 15961057]
 37. Lu Y, Hong S, Yang R, Uddin J, Gotlinger KH, Petasis NA, Serhan CN. Identification of endogenous resolvin E1 and other lipid mediators derived from eicosapentaenoic acid via electrospray low-energy tandem mass spectrometry: spectra and fragmentation mechanisms. *Rapid Commun Mass Spectrom* 2007;21:7–22. [PubMed: 17131464]
 38. Brooks JD, Milne GL, Yin H, Sanchez SC, Porter NA, Morrow JD. Formation of highly reactive cyclopentenone isoprostane compounds (A3/J3-isoprostanes) in vivo from eicosapentaenoic acid. *The Journal of biological chemistry* 2008;283:12043–12055. [PubMed: 18263929]
 39. Johnson EJ, Schaefer EJ. Potential role of dietary n-3 fatty acids in the prevention of dementia and macular degeneration. *Am J Clin Nutr* 2006;83:1494S–1498S. [PubMed: 16841859]
 40. Giacometti J, Milosevic A, Milin C. Gas chromatographic determination of fatty acids contained in different lipid classes after their separation by solid-phase extraction. *J Chromatogr A* 2002;976:47–54. [PubMed: 12462595]
 41. Schwarzenbach, G.; Irving, H. *Complexometric Titrations*. New York: Interscience; 1957.
 42. Davies SS, Amarnath V, Brame CJ, Boutaud O, Roberts LJ 2nd. Measurement of chronic oxidative and inflammatory stress by quantification of isoketal/levuglandin gamma-ketoaldehyde protein adducts using liquid chromatography tandem mass spectrometry. *Nat Protoc* 2007;2:2079–2091. [PubMed: 17853863]
 43. Nagata K, Suzuki H, Sakaguchi S. Common pathogenic mechanism in development progression of liver injury caused by non-alcoholic or alcoholic steatohepatitis. *J Toxicol Sci* 2007;32:453–468. [PubMed: 18198478]
 44. Lumeng L, Crabb DW. Alcoholic liver disease. *Curr Opin Gastroenterol* 2000;16:208–218. [PubMed: 17023878]
 45. Boutaud O, Montine TJ, Chang L, Klein WL, Oates JA. PGH₂-derived levuglandin adducts increase the neurotoxicity of amyloid beta1–42. *J Neurochem* 2006;96:917–923. [PubMed: 16412101]
 46. Crabb JW, Miyagi M, Gu X, Shadrach K, West KA, Sakaguchi H, Kamei M, Hasan A, Yan L, Rayborn ME, Salomon RG, Hollyfield JG. Drusen proteome analysis: an approach to the etiology of age-related macular degeneration. *Proc Natl Acad Sci U S A* 2002;99:14682–14687. [PubMed: 12391305]
 47. Ni J, Yuan X, Gu J, Yue X, Gu X, Nagaraj RH, Crabb JW. Study Group, C. Plasma protein pentosidine and carboxymethyllysine, biomarkers for age-related macular degeneration. *Mol Cell Proteomics*. 2009in press (PMID: 19435712)

48. Hageman GS, Luthert PJ, Victor Chong NH, Johnson LV, Anderson DH, Mullins RF. An integrated hypothesis that considers drusen as biomarkers of immune-mediated processes at the RPE-Bruch's membrane interface in aging and age-related macular degeneration. *Prog Retin Eye Res* 2001;20:705–732. [PubMed: 11587915]
49. Scholl HP, Charbel Issa P, Walier M, Janzer S, Pollok-Kopp B, Borncke F, Fritsche LG, Chong NV, Fimmers R, Wienker T, Holz FG, Weber BH, Oppermann M. Systemic complement activation in age-related macular degeneration. *PLoS ONE* 2008;3:e2593. [PubMed: 18596911]
50. Edelstein, C. General properties of plasma lipoproteins and apolipoproteins. In: Scanu, AM.; Spector, AA., editors. *Biochemistry of Plasma Lipoproteins*. New York: Marcel Dekker; 1990. p. 497
51. Heller JI, Crowley JR, Hazen SL, Salvay DM, Wagner P, Pennathur S, Heinecke JW. p-Hydroxyphenylacetaldehyde, an aldehyde generated by myeloperoxidase, modifies phospholipid amino groups of low density lipoprotein in human atherosclerotic intima. *The Journal of biological chemistry* 2000;275:9957–9962. [PubMed: 10744670]
52. Zieseniss S, Zahler S, Muller I, Hermetter A, Engelmann B. Modified phosphatidylethanolamine as the active component of oxidized low density lipoprotein promoting platelet prothrombinase activity. *The Journal of biological chemistry* 2001;276:19828–19835. [PubMed: 11278348]
53. White, DA. The phospholipid composition of mammalian tissues. In: Ansell, GB.; Hawthorne, JN.; Dawson, RMC., editors. *Form and Function of Phospholipids*. Amsterdam: Elsevier; 1973. p. 441-482.
54. de Kruijff B. Biomembranes. Lipids beyond the bilayer. *Nature* 1997;386:129–130. [PubMed: 9062183]
55. Schmidley JW, Dadson J, Iyer RS, Salomon RG. Brain tissue injury and blood-brain barrier opening induced by injection of LGE₂ or PGE₂. *Prostaglandins Leukot Essent Fatty Acids* 1992;47:105–110. [PubMed: 1461920]
56. Esterbauer H, Koller E, Snee RG, Koster JF. Possible involvement of the lipid-peroxidation product 4-hydroxynonenal in the formation of fluorescent chromolipids. *Biochem J* 1986;239:405–409. [PubMed: 3814081]
57. Chen JJ, Yu BP. Alterations in mitochondrial membrane fluidity by lipid peroxidation products. *Free Radic Biol Med* 1994;17:411–418. [PubMed: 7835747]
58. Iyer RS, Ghosh S, Salomon RG. Levuglandin E₂ crosslinks proteins. *Prostaglandins* 1989;37:471–480. [PubMed: 2762557]
59. Jain SK. The accumulation of malonyldialdehyde, a product of fatty acid peroxidation, can disturb aminophospholipid organization in the membrane bilayer of human erythrocytes. *The Journal of biological chemistry* 1984;259:3391–3394. [PubMed: 6706963]

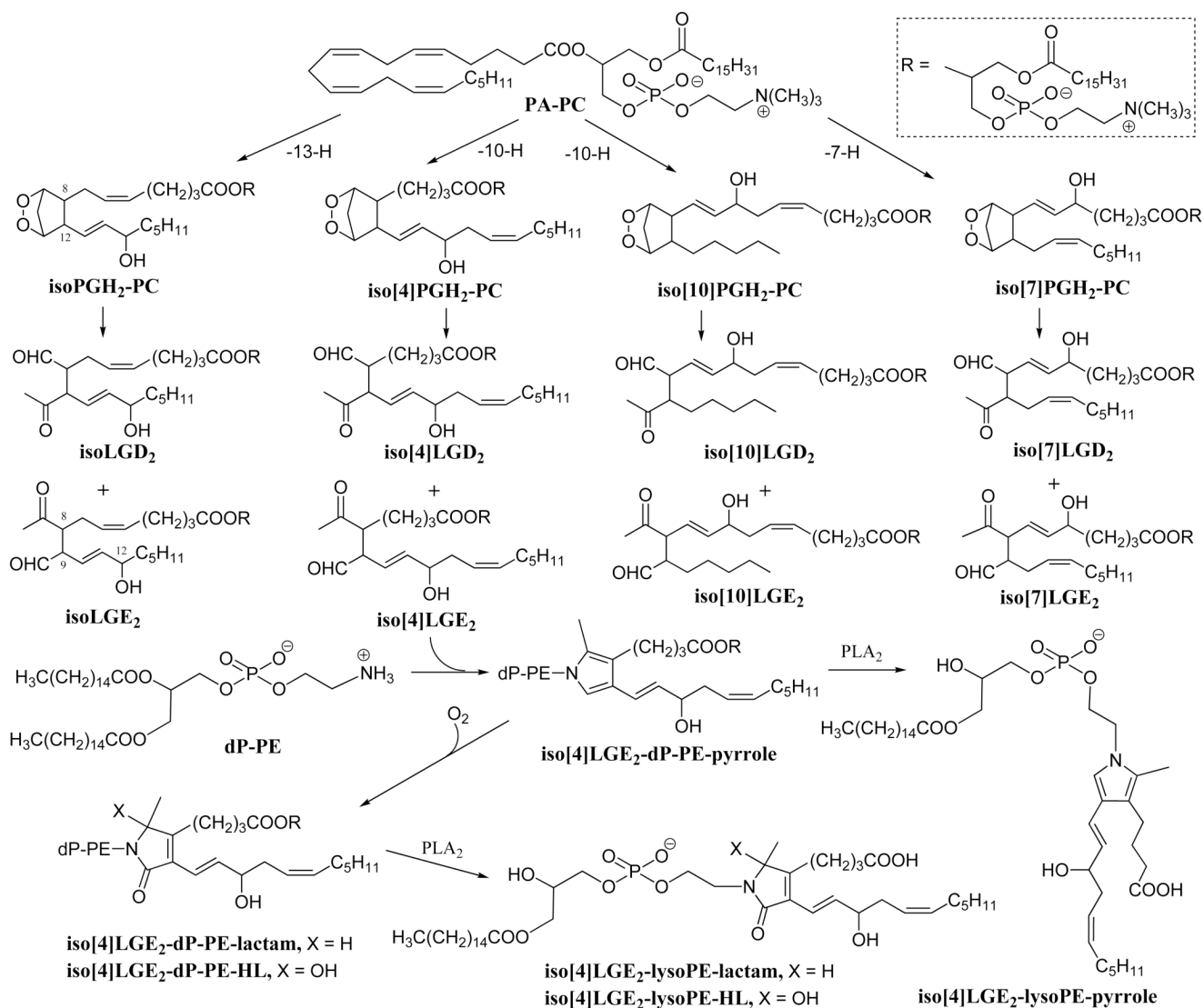


Figure 1.

Free radical-induced cyclooxygenation of PA-PC is postulated to generate a series of 8 structurally isomeric families each comprised of 8 isoLG stereoisomers through isoprostanoid endoperoxide intermediates. Two of these 64 different isomers, members of the isoLGE₂ and isoLGD₂ families of stereoisomers, are identical with products of the cyclooxygenase pathway, namely LGE₂ and LGD₂. Hydroxylactam (HL) end products, together with the corresponding lactams and pyrroles, are generated by the reaction of isoLGs with phosphatidylethanolamines. PLA₂-catalyzed selective lipolysis of these PE adducts converts them into the corresponding 2-lyso-PEs.

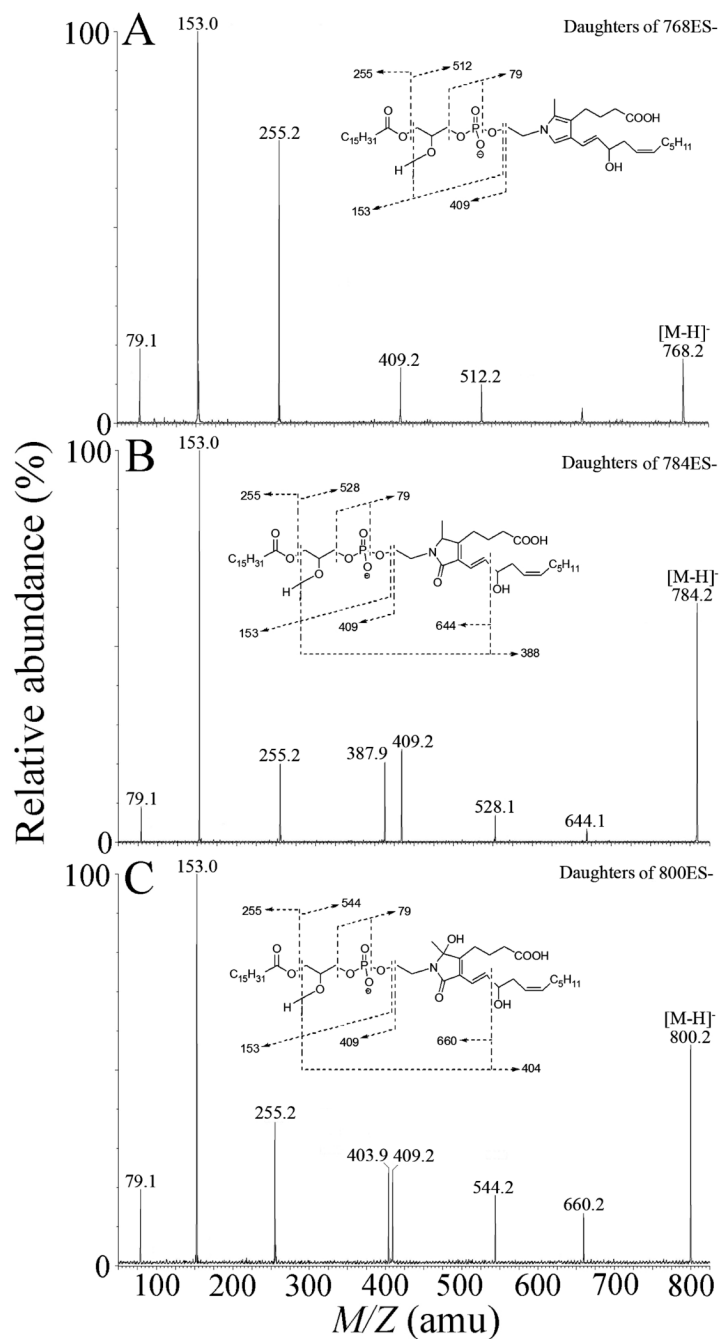


Figure 2. Collision-induced decomposition of electrospray-generated $[M-H]^-$ ions from iso[4]LGE₂-lysoPE adducts: (A) pyrrole adduct; (B) lactam adducts; (C) hydroxylactam adducts. Putative structures of the fragment ions are presented in the supplementary material figures S5 – S7.

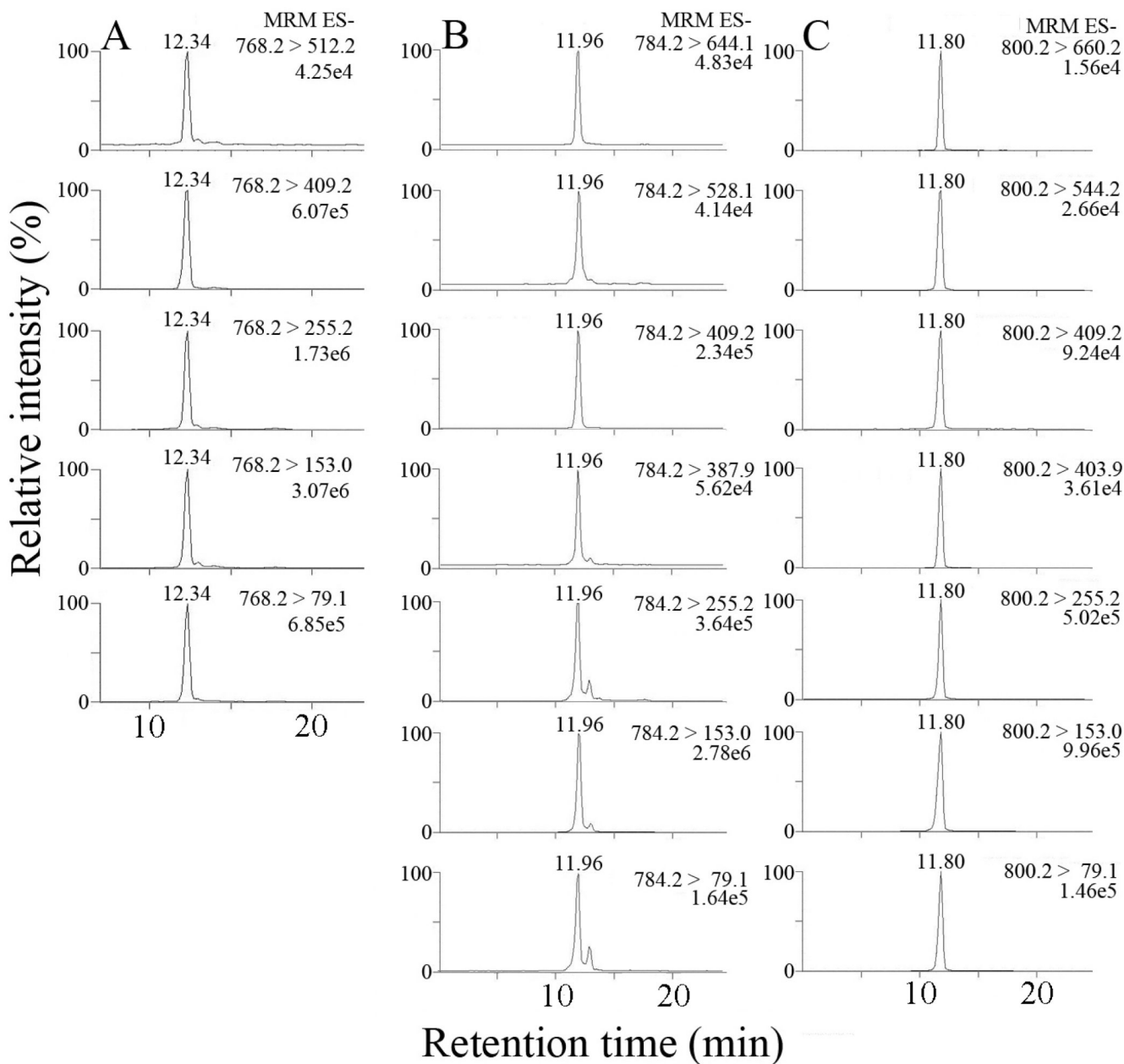


Figure 3.

LC/ESI/MS/MS analysis of iso[4]LGE₂-lysoPE adducts: (A) pyrrole adducts; (B) lactam adducts; (C) hydroxylactam adducts. In each case 5 transitions between parent and daughter ions common to all structural isomers were observed. For the lactam and hydroxylactam adducts, 2 transitions between parent and daughter ions diagnostic of the unique side chains of iso[4]LG structural isomers were also observed.

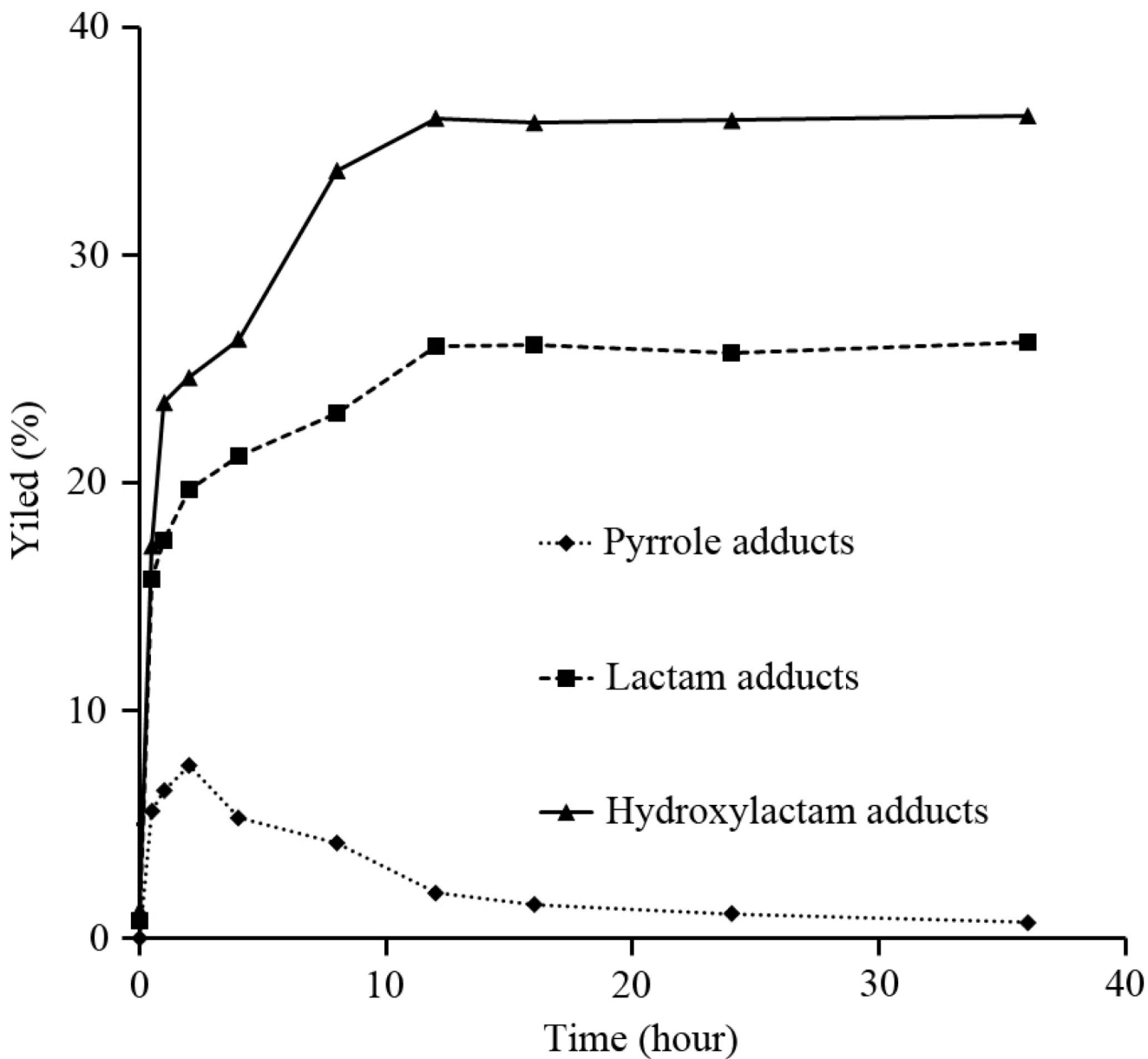


Figure 4.

Time course of formation of iso[4]LGE₂-lysoPE adducts using quantitation by LC/MS. Data are expressed as means of experiments (n = 3). The pyrrole yield climbs initially but then drops after 2 h owing to conversion into lactams and hydroxylactams.

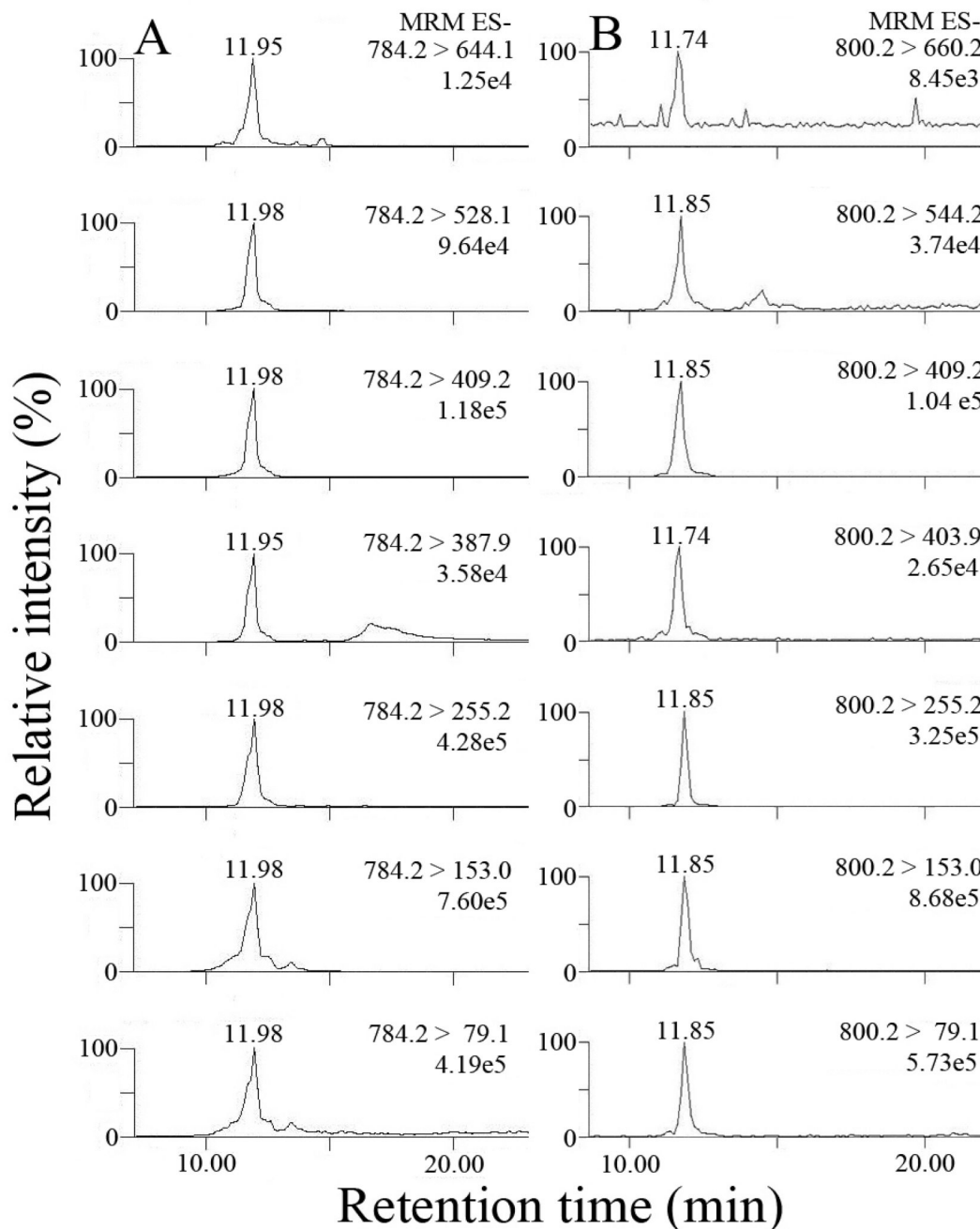


Figure 5.

LC/ESI/MS/MS analysis of putative iso[4]LGE₂-lysoPE adducts generated during oxidation of PA-PC *in vitro* by incubation with MPO/glucose-glucose oxidase/NO₂⁻ system and lysoPE followed by selective PLA₂-catalyzed hydrolysis of the adducts formed that releases isoLG-derived lactams and hydroxylactams from their esters with 2-lyso-PC: (A) lactam adducts; (B) hydroxylactam adducts.

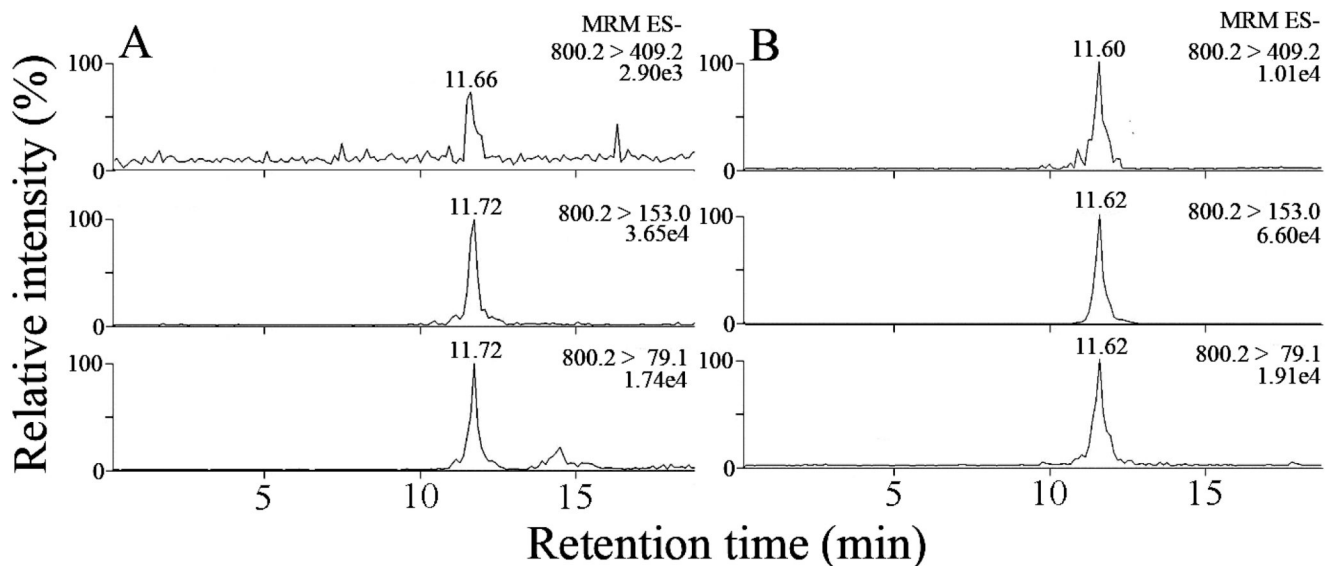


Figure 6.

LC/ESI/MS/MS analysis of isoLG-lysoPE-HL adducts derived from human plasma samples: (A) putative isoLG-lysoPE-HL adducts in lipid extract from human plasma after PLA₂ treatment; (B) synthetic standard of iso[4]LGE-lysoPE-HL adduct was spiked into and then extracted from human plasma without PLA₂ treatment that is required to release endogenous isoLG-lysoPE-HL adducts from their isoLG-PE-HL precursors.

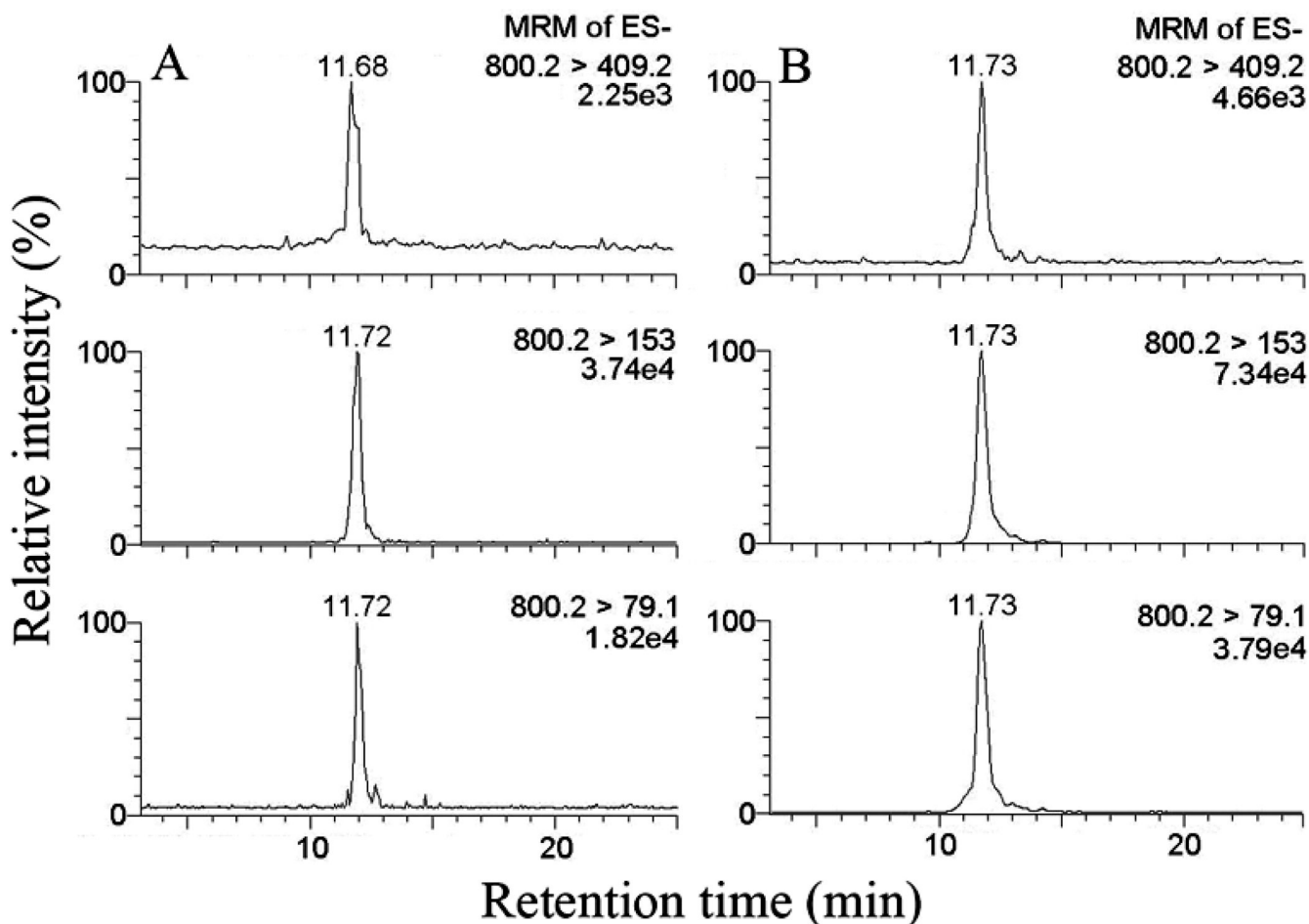


Figure 7.

(A) putative isoLG-lysoPE-HL adducts in lipid extract from human plasma after PLA₂ treatment; (B) lipid extract from human plasma after PLA₂ treatment – that releases endogenous isoLG-lysoPE-HL adducts from their isoLG-PE-HL precursors – spiked with authentic standard iso[4]LGE₂-lysoPE-HL (0.5 ng). The appearance of only single peaks in panel B supports the view that small retention time differences from one HPLC run to another are not evidence for nonidentity with isoLG-lysoPE-HL adducts.

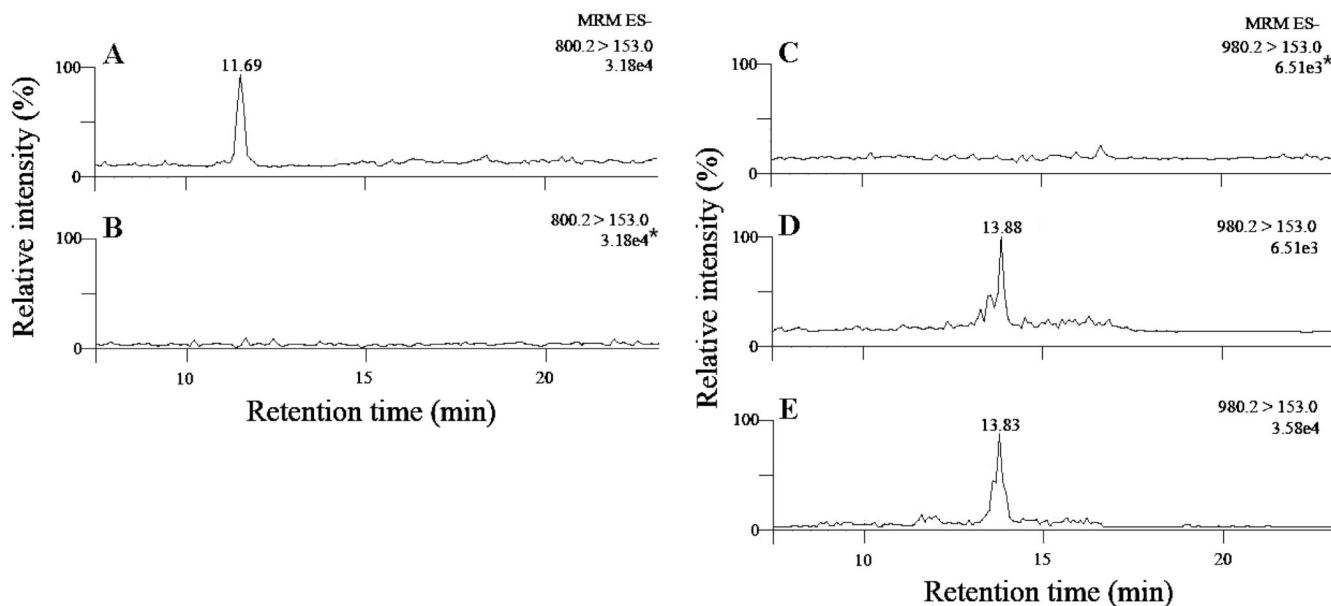


Figure 8.

LC/ESI/MS/MS analysis of putative isoLG-lysoPE-HL adducts in plasma extract with PLA₂ treatment before and after pentafluorobenzyl (PFB) esterification: (A) MRM for isoLG-lysoPE-HL before PFB derivatization; (B) MRM for isoLG-lysoPE-HL after PFB derivatization; (C) MRM for PFB derivative of isoLG-lysoPE-HL before PFB derivatization; (D) MRM for PFB derivative of isoLG-lysoPE-HL after PFB derivatization; (E) synthetic PFB derivative standard of iso[4]LG-lysoPE-HL adducts. In panel B, the intensity of the signal (3.18e4, with the asterisk) was obtained by normalizing to the intensity of the largest peak in panel A (3.18e4) from its original intensity 1.05e3. In panel C, the intensity of the signal (6.51e3, with the asterisk) was obtained by normalizing to the intensity of the largest peak in panel D (6.51e3) from its original intensity 1.26e3. In panels A, D and E, the intensities shown are the intensity of the largest peak in each chromatogram. The peak attributed to isoLG-lysoPE-HL disappears upon treatment with PFB-Br and a new peak appears corresponding to the expected PFB ester.

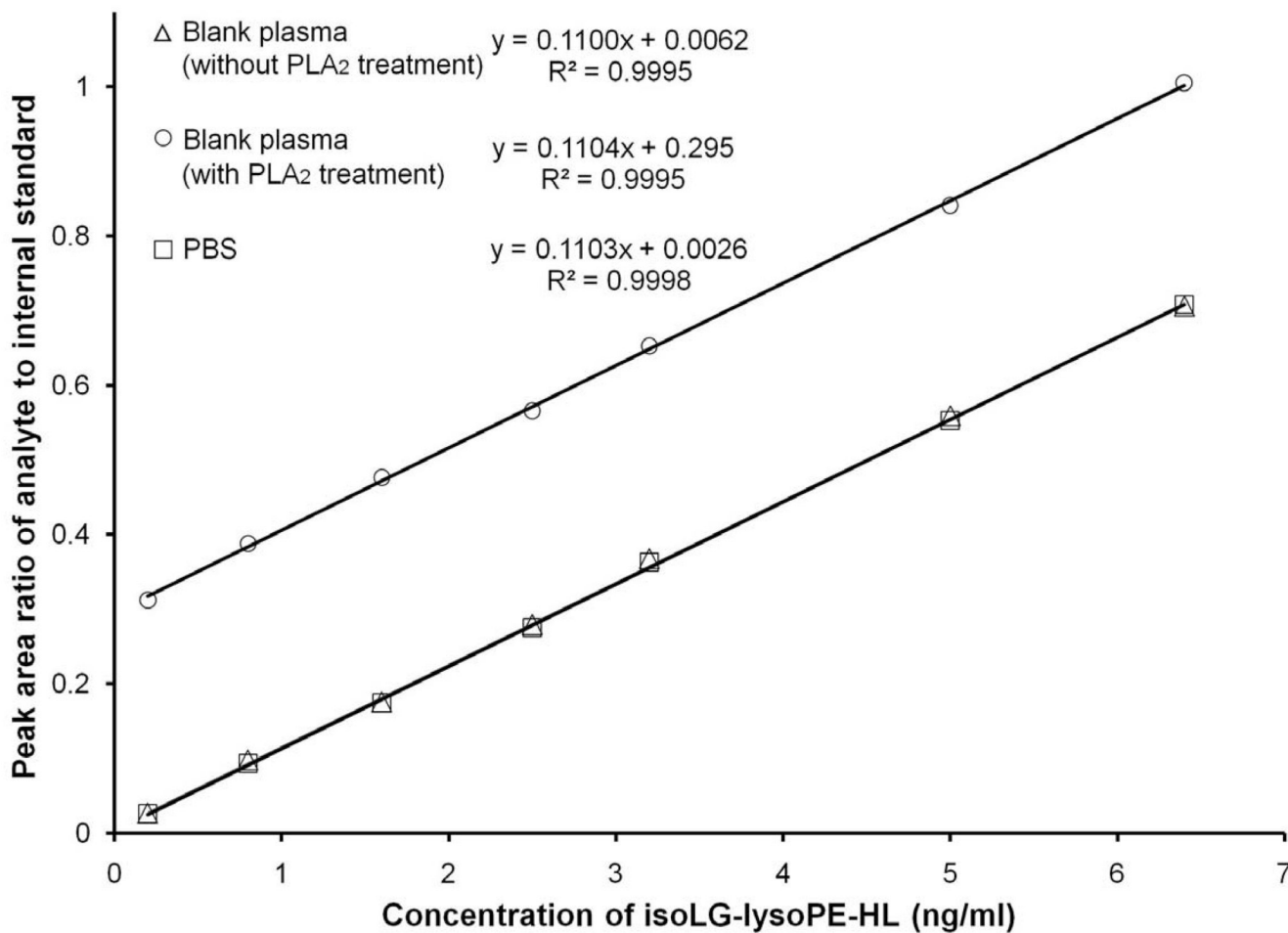


Figure 9. Calibration curves for iso[4]LGE₂-lysoPE-HL in blank plasma without PLA₂ treatment (Δ), in blank plasma with PLA₂ treatment (○) and in PBS (□). Data points represent the means of duplicate determinations from a representative experiment performed on 3 separate occasions. That plasma does not contribute a confounding matrix effect is supported by the superposition of the curves from blank plasma without PLA₂ treatment and from PBS. That iso[4]LGE₂-lysoPE-HL is released from endogenous lipids in plasma by PLA₂ treatment is supported by the elevated nonzero intercept of a parallel calibration curve obtained using plasma with PLA₂ treatment.

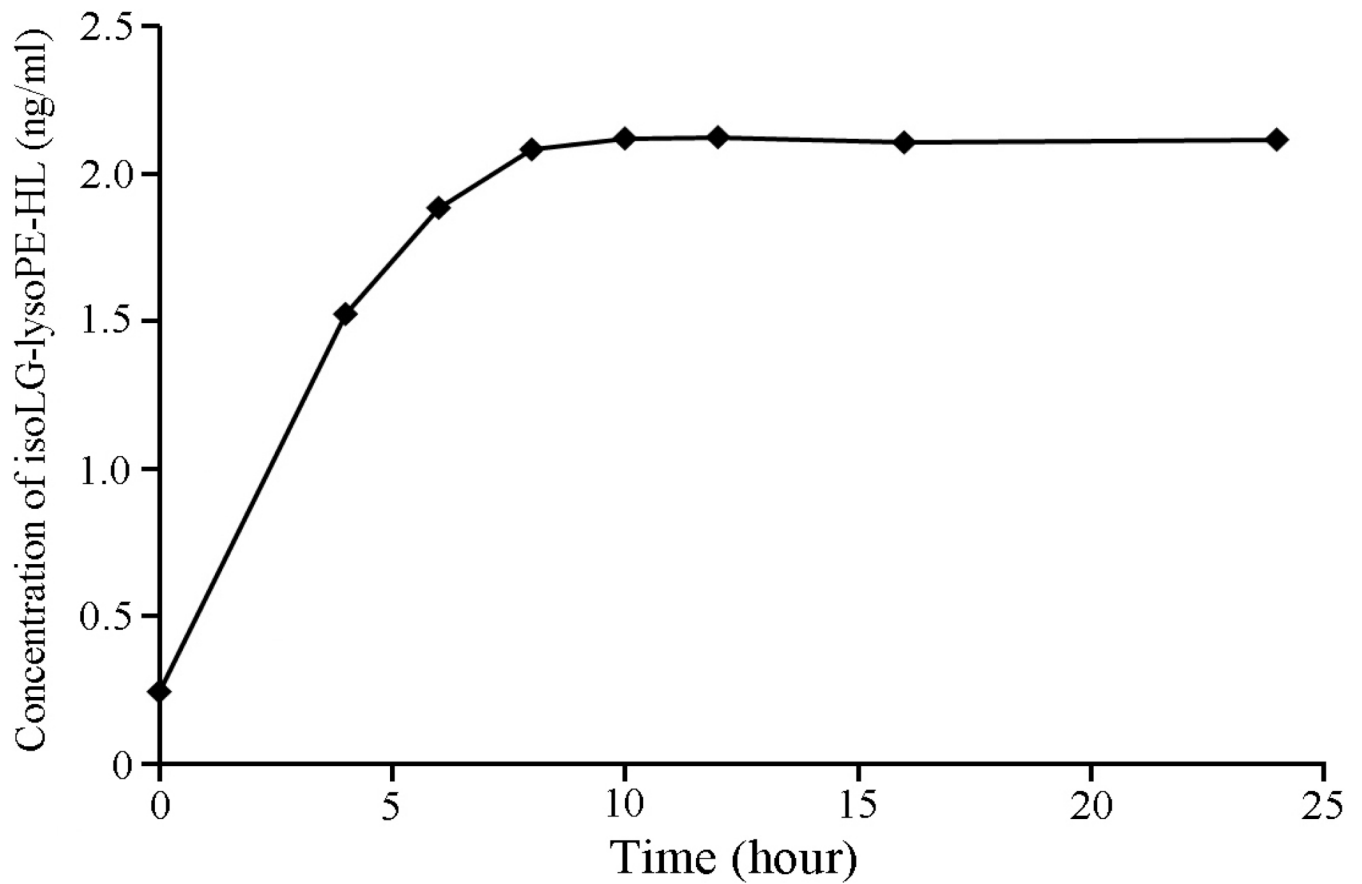


Figure 10. Time course of PLA₂ induced generation of isoLG-lysoPE-HL in lipid extracts from human plasma. Data points represent the means of duplicated determinations from a representative experiment performed on 3 separate occasions. Lipolysis goes to completion by 10 h at 37 ° C.

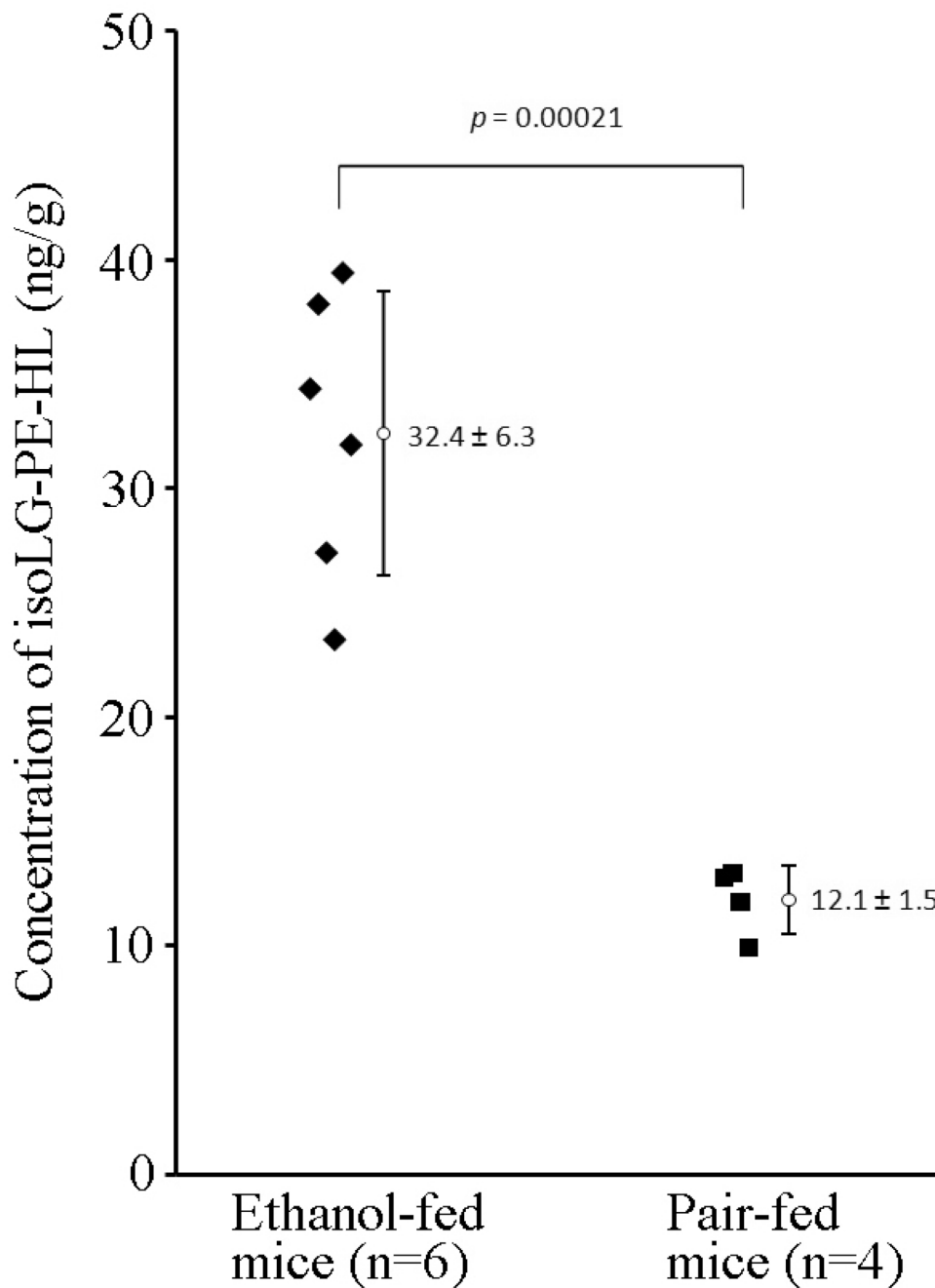


Figure 11.

Levels of isoLG-lysoPE-hydroxylactam adducts in mouse liver using LC-MS/MS. Liver samples were obtained from chronic ethanol (27% of calories for 4 weeks)-fed mice (C57BL/6 female, n = 6) compared to animals pair-fed diets which iso-calorically substituted maltose dextrins for ethanol (n = 4). Two-fold higher levels ($P = 0.00021$) were detected in livers from chronic ethanol-fed mice (32.4 ± 6.3 ng/g) compared to pair-fed mice (12.1 ± 1.5 ng/g).

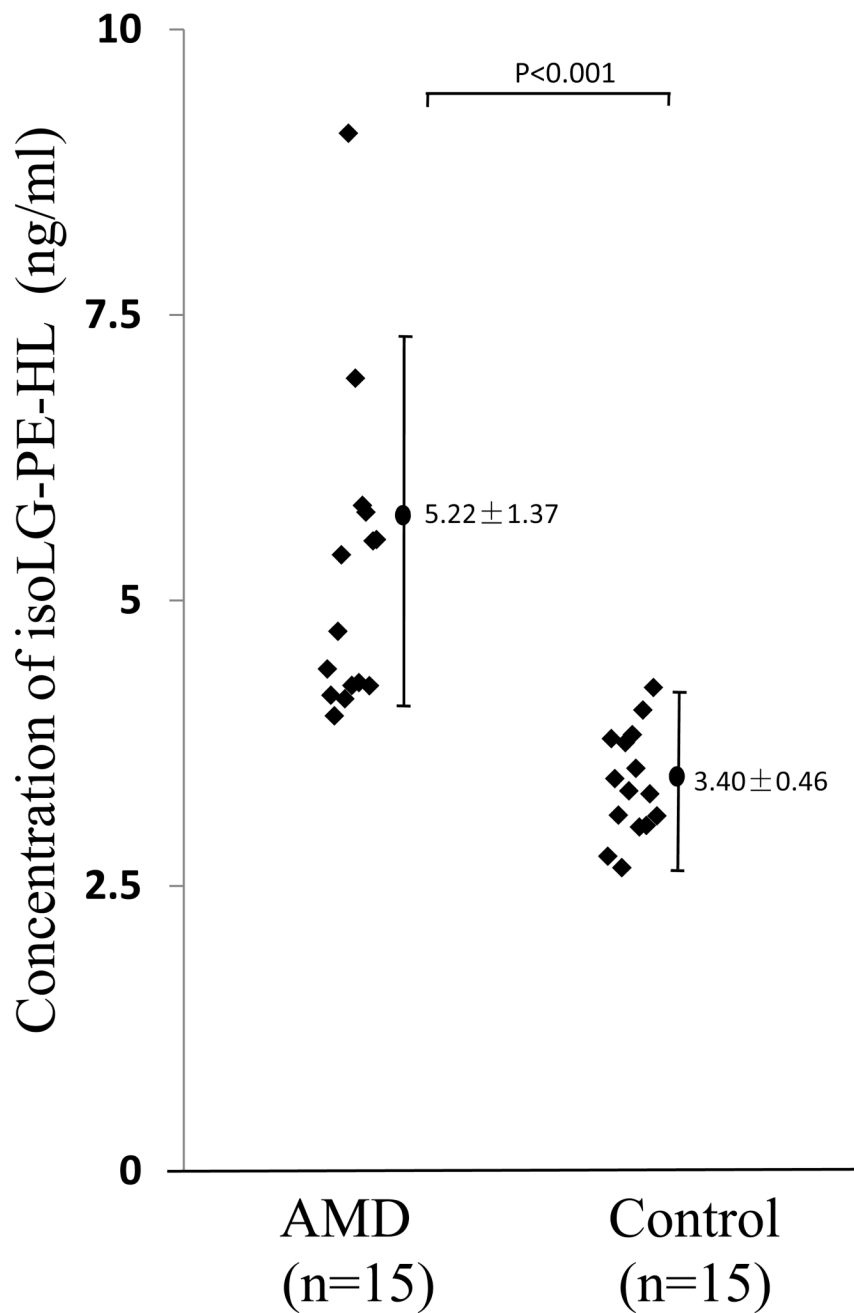


Figure 12.

Levels of isoLG-lysoPE-hydroxylactam adducts in human plasma quantified by LC-MS/MS. Plasma samples were obtained from 15 healthy normal donors (n = 15) and from patients with advanced age-related macular degeneration (n = 15). The mean level detected in age-related macular degeneration plasma (5.2 ± 0.4 ng/ml, n = 15 patients) was significantly elevated ($P < 0.0001$) compared with plasma from healthy volunteers (3.4 ± 0.1 ng/ml, n = 15).

Table 1

Replicated analyses of different plasma samples with PLA₂ treatment. (control samples of AMD study, n = 5)
Data points represent the means of duplicated determinations from a representative experiment performed on 3 separate occasions.

Plasma samples	Calculated Concentration (ng/mL) (mean ± SD)	Intra-day CV (%)	Inter-day CV (%)
C1	2.76 ± 0.13	3.13	4.71
C2	3.79 ± 0.21	2.15	5.54
C3	3.44 ± 0.18	2.32	5.23
C4	3.12 ± 0.16	2.85	5.13
C5	2.66 ± 0.14	2.65	5.26

Table 2

Blank plasma samples (n = 5) spiked with known amounts (2.5 ng/ml or 5 ng/ml) of iso[4]LGE₂-lysoPE-HL (omit addition of PLA₂ and CaCl₂ during PLA₂ treatment to avoid the generation of additional isoLG-lysoPE-HLs from endogenous phospholipids in plasma). Inter-day study was conducted in 3 days. Data points represent the means of duplicated determinations from a representative experiment performed on 3 separate occasions.

Nominal Concentration (ng/mL)	Calculated Concentration (ng/mL) (mean ± SD)	Intra-day CV (%)	Inter-day CV (%)	Accuracy (%)
2.5	2.45 ± 0.11	2.12	4.49	-2.00
5.0	4.88 ± 0.26	3.15	5.32	-2.40